APPLICATIONS OF NON - LINEAR MICRO RING RESONATORS

WEERAPHAN SIRIRITH

A THESIS SUBMITTED IN PARTIAL FULFILLMENT

OF THE REQUIREMENT FOR THE DEGREE OF

DOCTOR OF ENGINEERING IN ELECTRICAL ENGINEERING

FACULTY OF ENGINEERING

KING MONGKUT'S INSTITUTE OF TECHNOLOGY LADKRABANG

2010

KMITL–2010–EN–D–018-005

หัวข้อวิทยานิพนธ์	การประยุกต์ของวงแหวนโพรงสั่นพ้องขนาดเล็กชนิดไม่เป็นเชิงเส้น
นักศึกษา	นายวีรพันธุ์ ศิริฤทธิ์
รหัสประจำตัว	46060009
ปริญญา	วิศวกรรมศาสตรดุษฎีบัณฑิต
สาขาวิชา	วิศวกรรมไฟฟ้า
พ.ศ.	2553
อาจารย์ที่ปรึกษาวิทยานิพนธ์	รศ.ดร. สมศักดิ์ มิตะถา

บทคัดย่อ

วิทยานิพนธ์นี้นำเสนอการประยุกต์ของอุปกรณ์ชนิดไม่เป็นเชิงเส้นโดยใช้วงแหวนโพรงสั่นพ้องขนาดเล็กเพื่อใช้ในการเข้ารหัสดีเอ็นเอซึ่งสามารถประยุกต์ใช้กับการส่งข้อมูลลับและการติดต่อแบบไร้สาย วิทยานิพนธ์นี้ได้นำเสนองานวิจัยแบ่งออกเป็น 4 หัวข้อดังนี้

หัวข้อแรกนำเสนอการออกแบบระบบการป้องกันที่ใช้พฤติกรรมที่ไม่เป็นเชิงเส้นของโซลิตอนแบบมืดและแบบสว่างผ่านวงแหวนโพรงสั่นพ้องขนาดเล็กสำหรับการประยุกต์ใช้ในสัญญาณการป้องกัน หัวข้อที่สองนำเสนอการนำสัญญาณแถบความถี่กว้างมากมาใช้ด้วยพัลส์โซลิตอนผ่านตัวกลางที่ไม่เป็นเชิงเส้นชนิดเดอร์ ผลลัพธ์ที่ได้แสดงให้เห็นถึงศักยภาพในรูปของการสร้าง ขยาย กักเก็บ และสร้างใหม่ของสัญญาณแสงแถบความถี่กว้าง หัวข้อที่สามเสนอวิธีการเข้ารหัสดีเอ็นเอของสัญญาณไม่เป็นเชิงเส้น และสัญญาณนี้สามารถแปลงเป็นรหัสลอจิกพัลส์ A หรือ T หรือ C หรือ G โดยวิธีควอนไตซ์สัญญาณ สุดท้ายเป็นการเสนอระบบการป้องกันข้อมูลสวิทช์ชิ่งกลุ่มอย่างสูงสุด โดยอาศัยพฤติกรรมที่ไม่เป็นเชิงเส้นของโซลิตอนในโพรงสั่นพ้องวงแหวนขนาดเล็ก การสร้างสัญญาณไม่เป็นเชิงเส้นกำเนิดจากพฤติกรรมที่ไม่เป็นเชิงเส้นที่เรียกว่าปรากฏการณ์ของเดอร์ การควบคุมกำลังอินพุทและพารามิเตอร์บางตัวของอุปกรณ์สามารถกำหนดคุณลักษณะของสัญญาณเอาท์พุทได้ ผลลัพธ์ที่ได้แสดงให้เห็นถึงศักยภาพของอุปกรณ์เพื่อป้องกันสัญญาณที่มีลักษณะเป็นกลุ่มข้อมูล

Thesis Title	Applications of Non - Linear Micro Ring Resonators
Student	Mr. Weeraphan Siririth
Student ID.	46060009
Degree	Doctor of Engineering
Program	Electrical Engineering
Year	2010
Thesis Advisor	Assoc. Prof. Dr. Somsak Mitatha

ABSTRACT

This thesis presents the interesting results for application of the nonlinear device known as a nonlinear micro ring resonator to process the DNA codes which can be applied to the secured data transmission and wireless links applications.

We propose four topics. Firstly, we propose a design of a security scheme by using the nonlinear behaviors of temporal dark and bright solitons within a micro ring resonator system for signal security application. Secondly, we propose the large bandwidth signal generated by using a soliton pulse propagating within a Kerr type nonlinear medium. The results have shown the potential of using such system for broadband light source generation, amplification, storage and regeneration. Thirdly, we propose DNA encoding of nonlinear signals in nonlinear micro ring resonator. The generated nonlinear signals can be formed as the logical pulses "A" or "T" or "C" or "G" using the signal quantizing method. Finally, we propose a system of the high secured packet switching using the nonlinear behaviors of soliton in a micro ring resonator. The nonlinear signals are generated by a Kerr effects nonlinear type, where the control input power or device parameters can be used to specify the output signals. Results obtained have shown the potential of using such a proposed device, in which the packet switching data can be performed and secured.

ACKNOWLEDGEMENTS

Firstly of all, I would like to express my guidance sincere gratitude to my advisor, Assoc. Prof. Dr. Somsak Mitatha, for his attention, insight, encourage, guided, and support during this research and for being available at anytime to response my questions, which has been valuable. I am grateful to Assoc. Prof. Dr. Preecha Yupapin for introducing me the research topics, for the many insightful conversational, and his constant encouragement. Working with him has been a great learning experience.

I would also like to thank every young members of the Advanced Research Center of Photonic Laboratory (ARCP) of the Department of Applied Physice, Faculty of Science, KMITL; whose support has created a friendly environment.

I would also like to thank every young members of the Hybrid Computing Research Laboratory (HCRL) of the Department of Computer Engineering, Faculty of Engineering, KMITL; whose support has created a friendly environment.

I would like to thank my committee members, Assoc. Prof. Dr. Suripon Somkuarnpanit, Assoc. Prof. Dr. Athikom Roeksabutr, Assoc. Prof. Dr. Pitikhate Sooraksa, Assoc. Prof. Dr. Preecha Yupapin, for their assistance, helpful comments, and insightful suggestions.

Finally, my greatest thanks are to my beloved family whose caring, understand, and possible attitude have encouraged me to go forward during difficult times. Whose never-ending love and support made the completion of this work completed and my dream of a graduate education come true.

Weeraphan Sririth

CONTENTS

Pages

CONTENTS (cont.)

LIST OF FIGURES

Figures **Pages**

LIST OF FIGURES (cont.)

Figures **Pages**

LIST OF FIGURES (cont.)

Figures **Pages**

CHAPTER 1

INTRODUCTION

1.1 The Optical Network

Optical ring resonator have numerous applications in signal processing, laser systems, industrial sensing, optical communication, interferometers, etc. They can be fabricated using bulk optical element (mirror and beam splitter), fiber optic component or integrated optics technology. Regarding their geometry there are not necessarily circular in shape. Integrated optical technology allows for extreme miniaturization, for the fabrication of rings with very perimeters, approaching dimensions commensurate with the wavelengths used in hi-speed communication systems.

The use of light for communication purposes dates back to the use of smoke and fire to convey a piece of information, such as a victory in a war. There are many reasons that made photons more popular to use in information processing. Photons are able to accomplish certain functions better than electrons by virtue of their special properties. The very large bandwidth, ~10^{15} Hz, gives optics a potential speed for signal processing which is well beyond any electronics. Indeed, the shortest optical pulses of <10fs give light three order of magnitude advantage over the shortest electrical pulse [1]. When it comes to interconnect on a chip, the wiring capacitance will set the speed limits of integrated circuits. Besides, photons can pass through each others unperturbed in the absence of a nonlinear interaction, whereas electrons interact with each other even at a distance.

The turn of the new millennium witnessed an explosion in data-traffic volume, due to the ongoing increasing demand on the Internet. Therefore, all-optical switching devices have been looked at as key components for future high-speed optical communication systems. Such devices would enable highly parallel logic operations as well as ultrafast switching because of the instantaneous nature of virtual optical transitions [2]. With the recent advances in semiconductor fabrication, there has been a noticeable effort to bring those devices on semiconductor platforms to the real world. An ideal all-optical switch is the one that poses the following characteristics. It would only require as little as sub picojoule of energy to switch with at least 20dB switching contrast. Beside compactness, it is desirable to integrate such a device with already established optoelectronics devices on a planar integrated photonic circuit. One category of devices that has a great potential to meet those requirements is ***microring resonators.***

1.2 Optical Signal Processing using Nonlinear Optics

Networking applications such as data browsing, large file transfer, multimedia-on-demand, and videoconferencing require high quality transfer of data streams of different lengths and initial formats. Optical fiber provides a suitable medium in which it is possible to reach tremendous transmission rates over long distances [3]. The maximum information carrying capacity was estimated to be around 100 THz [4]. Very high data rates can be achieved using a combination of wavelength- and time-division multiplexing techniques (WDM and TDM). WDM involves sending many signals in parallel at closely spaced wavelengths along the same fiber, while TDM allows close spacing in time of bits in a single channel.

While there exist means to produce, transfer, and detect information at a very high bandwidth, there is a need for more agility in photonic networks. The agility of present-day optical networks is limited by the electronic nature of a very important function: the processing of data signals. Signal processing is responsible for switching and routing traffic, establishing links, restoring broken links, testing, and managing the network.

At present, important and functionally complex signal processing operations of switching and routing are carried out electronically. Electronic signal processing imposes two significant limitations on the functionality of optical networks: cost and opacity. Today, signal switching and routing requires converting the optical information into electrical signals, processing in the electronic domain, and converting back to the optical domain before retransmission. Such an operation requires detection, retiming, reshaping, and regeneration at each switching and routing point. This necessitates complex and expensive electronic and electro-optical hardware at each routing and switching node.

The use of electronic signal processing places strict requirements on the format of data streams transferred and processed, thus making the signal processing opaque. Repetition rates of optical signals, power levels, and packet lengths have to be standardized before they can be processed electronically. In addition, since modern electronics can process information at repetition rates far below the fundamental limits of the optical transmission, electronics imposes limits on the ultimate transmission rate of a network.

The ability to perform signal processing operations entirely within the optical domain would eliminate the requirement of optical-electrical-optical conversions, while providing the agility and speed inherent to optical elements. Provisioning of services with a vast diversity of rates and duration of connections could be enabled. All-optical switching solutions would be transparent to bit rate and protocols. The speed of electronic devices would no longer limit network throughput: optical signal processing, in contrast with electronics, may provide ultrafast subpicosecond switching times [5].

In contrast to the optical signal processing solutions discussed in the previous section, nonlinear optics can potentially support transparent and fast self-processing of signals. A variety of nonlinear optical signal processing functions can be realized with similar fundamental building blocks [6–8]. Nonlinear optical elements and devices can be either integrated in photonic circuits [9] or used in a free-standing configuration [10].

Nonlinear optics can enable signal processing without the requirement of external electrical, mechanical, or thermal control [11]. The response time of properly designed nonlinear optical devices is limited fundamentally only by the nonlinear response time of the constituent materials [5, 12–14]. Photons do not interact with each other *in vacuo*. In order to perform nonlinear optical signal processing operation the properties of a medium through which the light travels must be modified by the light itself. Optical signals then propagate differently as a result of their influence on the medium.

Nonlinear optical signal processing elements utilize the illumination-dependent real and imaginary parts of the index of refraction [11]. Depending on the material and spectral position, the refractive index and absorption of a given nonlinear material can either increase or decrease with increasing illumination. A wide range of broadband and wavelength-selective nonlinear optical signal processing devices has been proposed and demonstrated.

The most commonly studied nonlinear optical switching elements are nonlinear Fabry-Perot interferometers, nonlinear Mach-Zehnder modulators, nonlinear directional couplers, optical limiters, and nonlinear periodic structures. A nonlinear Fabry-Perot interferometer consists of two mirrors separated by a nonlinear material. As the refractive index of the nonlinear material changes with an increased level of illumination, the effective path length of the resonator is altered. A nonlinear Fabry-Perot interferometer can be tuned out of, or into, its transmission resonance. When illuminated with the continuous-wave light, a nonlinear Fabry-Perot interferometer can exhibit

optical bistability. Optical bistability is a phenomenon in which the instantaneous transmittance of the device depends both on the level of incident illumination and on the prior transmittance of the device. Such an element enables all-optical memory.

In a nonlinear Mach-Zehnder modulator and a nonlinear directional coupler, a part of the waveguide is made out of a nonlinear material. Changing the intensity of the incident light changes the effective path length experienced by the light. This, in turn, through phase interference, results in an illumination-dependent transmittance in a Mach Zehnder modulator, and an illumination-dependent coupling in a nonlinear directional coupler.

A number of techniques use nonlinear properties of materials to obtain power limiting, and associated with it, on-off switching. Such devices are based on total internal reflection [15], self-focusing [16], self-defocusing, or two photon absorption [17]. Nonlinear periodic structures combine the phenomena of nonlinear index change and distributed Bragg reflection. The intensity-dependent transmission and reflection properties of nonlinear periodic structures can be harnessed to yield various signal processing functions. Prior to this work it has been demonstrated that nonlinear periodic structures can support optical switching, optical bistability, and soliton propagation of pulses. Nonlinear periodic structures offer many structural and material degrees of freedom allowing modification of the general character and specifics of their optical response.

1.3 Chaos in Communication

Chaos communications is an application of chaos theory which is aimed to provide security in the transmission of information performed through telecommunications technologies. By secure communications, one has to understand that the contents of the message transmitted are inaccessible to possible eavesdroppers.

In chaos communications security (i.e., privacy) is based on the complex dynamic behaviors provided by chaotic systems. Some properties of chaotic dynamics, such as complex behaviors, noise-like dynamics (pseudorandom noise) and spread spectrum, are used to encode data. On the other hand, being chaos a deterministic phenomenon, it is possible to decode data using this determinism. In practice, implementations of chaos communications devices resort to one of two chaotic phenomena: synchronization of chaos, or control of chaos. The implement chaos communications using such properties of chaos, two chaotic oscillators are required as a transmitter

(or master) and receiver (or slave). At the transmitter, a message is added on to a chaotic signal and then, the message is masked in the chaotic signal. As it carries the information, the chaotic signal is also called chaotic carrier.

When chaos synchronization is used, a basic scheme of a communications device is made by two identical chaotic oscillators. One of them is used as the transmitter, and the other as the receiver. They are connected in a configuration where the transmitter drives the receiver in such a way that identical synchronization of chaos between the two oscillators is achieved. For the purpose of transmission of information, at the transmitter, a message is added as a small perturbation to the chaotic signal that drives the receiver. In this way, the message transmitted is masked by the chaotic signal. When the receiver synchronizes to the transmitter, the message is decoded by a subtraction between the signal sent by transmitter and its copy generated at the receiver by means of the synchronization of chaos mechanism. This works because, whilst the transmitter output contains the chaotic carrier plus the message, the receiver output is made only by a copy of the chaotic carrier without the message. The electrical signals with a power far below the one produced by the chaotic system itself. Thus, the complexity of chaos and its sensitivity to small perturbations can be combined harmoniously by using the sensitivity to control (and take advantage of) the complexity. As a consequence, it is currently recognized by many engineers that the fact that chaos provides complex behavior from simple systems can be exploited to obtain technological advantages over conventional means for information transmission.

Chaos has been regenerated as a nonlinear property in the areas such as mathematics [18], physics [19], electronics and communication [20].Most of them have reported the nonlinear properties can be accorded when the concerned parameters are suitable in same cases, which is commonly known as a non-periodic behavior and become a penalty of the system. However, the benefit of such a property can also be accepted, Chaotic communication has recently attracted great interest because of its potential applications in secure communications and the secretly communications [20].

Secure communication systems based on chaos in ring resonator were proposed and studied with message coding, various schemes were proposed and the nonlinear effect of the coding process [21] and control chaotic signal encoding were studied consist of 3 cases, which 1) control input power(mW) 2) control threshold power (mW) and 3) control range of roundtrip time. The chaotic coding consist of the methods are Sampling [22],Quantizing [23],Chaos Synchronization [24]and

chaotic message encoding communication with chaos [25].The chaotic signal encoding could be application in the military message transmission.

1.4 DNA Code and High Security Packet Switching

In recent years, semiconductor micro ring resonators have received great interest as potential building blocks for optoelectronic integrated circuits due to their ultra compactness and small size, which can lead to high device integration densities. Moreover, the field buildup inside the ring cavity can be used for all optical signal processing functions based on enhanced nonlinear effects [26]. In principle, the DNA coding methods are processed by sampling, quantizing, and synchronization. In this paper, we have proposed the extended details of our previous work [27], where the other point of view from its applications is the optical output which can be formed by the DNA codes. The selected input signals can be used to control the required DNA encoding, which can be distributed into the wavelength router or optical wireless link. These can be applied into the optical networks to encrypt and the required communication data can be retrieved. The ring parameters used are based on the practical device parameters as shown in references [28, 29]. Simulation results obtained have shown the potential of application for secure wireless link in the optical networks. The basic theory of a microring resonator is reviewed, the DNA quantizing and coding and control are presented in detail.

Moreover, the field buildup inside the ring cavity can be used for all optical signal processing functions based on enhanced nonlinear effects [26]. In principle, the DNA coding methods are processed by sampling, quantizing, and synchronization. In this paper, we report the design of packet switching and application for the DNA codes generation using the nonlinear behaviors of light in the micro ring resonators, where three forms of applications for chaotic signal, encoding, and packet switching are proposed and discussed. The selected input signals can be used to control the required DNA encoding, which can be distributed into the wavelength router or optical wireless link. These can be applied into the optical networks to encrypt and the required communication data can be retrieved. The ring parameters used are based on the practical device parameters as shown in references [28, 29]. Simulation results obtained have shown the potential of application for secure wireless link in the optical networks, where the high security packet

switching data can be performed. The basic theory of a micro ring resonator is reviewed, the DNA quantizing and coding and control are presented in detail.

1.5 Goal of the Thesis

For the benefit of nonlinearity penalty of light, the nonlinear behavior consists of the Kerr effect, chaotic, bistability and bifurcation. Which the chaos can be utilized to the chaos communications. It is an application of Chaos theory which is aimed to provide security system in the transmission of information performed through telecommunications technologies. By secure communications, one has to understand that the contents of the message transmitted are inaccessible to possible eavesdroppers.

Micro ring resonators with these applications are thus need careful and exact design for their correct operation. A direct result of the progress in fabrication techniques is the increased need of the accurate models for characterizing the nonlinear devices. For very simple devices, analytical tools provide a framework for quick low cost feasibility studies and allow for design optimization before devices are fabricated.

The primary goal of this thesis investigates the design and simulation nonlinear characteristics of ring resonator architectures based on material of InGaAsP/InP. Second goal is to design of the temporal dark-bright solitons conversion system and storage and tunable light source generated by a soliton pulse. Third goal is to generate DNA Code using bifurcation nonlinear in a micro ring resonator for optical packet switching application. Fourth goal is to design of the secured packet switching using the Kerr effects nonlinear type of soliton in a micro ring resonator for communication security application. Finally, is to generate the logical pulses "A" or "T" or "C" or "G" by using the chaotic signal quantizing method, which the chaotic signal to be the DNA code and the high security packet switching in optical wireless links.

1.6 Scope of the Thesis

With the growing importance of micro ring resonators for a variety of applications, it becomes necessary to devise a model which is directly interpretable in physical terms, and which is essentially free of any fit parameters. In this thesis, fine the new technique application to the coupled multiple ring resonators add/drop filters and analyze the filtering characteristics in general.

In this thesis, the chaos signal cancellation approach to design and analyze nonlinear optical add/drop filters. We created the DNA code for secure communications and performed and modulated the generated carrier within the ring system. The DNA codes can be generated and formed by the logical pulses "A" or "T" or "C" or "G" by using the chaotic signal quantizing method, which the chaotic signal to be the DNA code and the high security packet switching in optical wireless links.

1.7 Organization of the Thesis

This thesis presents a novel simulation and a novel design in application micro ring resonator. The organization is as follows:

The current chapter gives an introduction to the subject of the thesis and generalized signal processing in optical wireless links.

Chapter 2 describes some of phenomena of nonlinear optics.

Chapter 3 discusses analytical approach of signal processing which is used to characterize nonlinear devices in micro ring resonator.

Design nonlinear devices by using nonlinear behavior in micro ring resonator and all essential parameters describing the nonlinear characteristics are extracted in chapter 4 and 5.

Finally, Chapter 6 presents a summary of the results of the thesis and a discussion of future research.

CHAPTER 2

PHENOMENA OF NONLINEAR OPTICS

The use of semiconductor materials as nonlinear optical elements bridges the gap between optics and electronics. It opens the possibility for integrating the laser sources, signal processing elements, and detectors on the same platform. In this regard, the III-V binary semiconductors, such as GaAs and InP, have acquired great attention in the last few decades because they are direct band gap materials and possess higher nonlinear coefficients than their competing materials. Another attractive feature of binary semiconductors is that they can be combined or alloyed to form ternary or quaternary compounds. Doing so, this makes it possible to vary the band gap of the material continuously together with its band structure, electronic, and optical properties. As an example, the band gap energy of the ternary compound $Al_xGa_{1-x}As$ depends on the mole fraction x. Another important quaternary compound that we will consider is $In_{1-x}Ga_xAs_yP_{1-y}$. Therefore, one can design ternary and quaternary compounds to be transparent for optical channel waveguides or active for lasers and amplifiers at the 1550 nm communication window.

In this chapter, we will discuss different nonlinear processes that affect the performance of semiconductor micro ring resonators as all-optical signal processing tools.

2.1 Nonlinear Susceptibility

Nonlinear optics is the study of phenomena that occur as a consequence of the modification optical properties of a material under intense illumination. Typically, only laser light is sufficiently intense to modify the optical properties of a material. Nonlinear optical phenomena are nonlinear in the sense that the induced material polarization is nonlinear in the electric field [30,31]. The general equation that describes the optical field evolution in a dielectric material is given by

$$\nabla^2 \mathrm{E} - \frac{1}{c^2}\frac{\partial^2 \mathrm{E}}{\partial t^2} = -\mu_0 \frac{\partial^2 \mathrm{P(E)}}{\partial t^2} \tag{2.1}$$

Where the polarization $\vec{P}$ characterizes the medium and it is a function of the electric field. In the case of weak nonlinear behavior of the medium, the polarization can be expressed by a Taylor polynomial as

$$\vec{P} = \underbrace{\varepsilon_0 \vec{E} + \varepsilon_0 \chi^{(1)} : \vec{E}}_{linear\ P_L} + \underbrace{\varepsilon_0 \chi^{(2)} :: \vec{E} \cdot \vec{E} + \varepsilon_0 \chi^{(3)} ::: \vec{E} \cdot \vec{E} \cdot \vec{E} + \ldots}_{nonlinear\ P_{NL}}, \tag{2.2}$$

Where dielectric dispersion is ignored. $\chi^{(1)}$ is the linear susceptibility, :represents the inner tensor product and the second and the third-order tensor $\chi^{(2)}$ and $\chi^{(3)}$ are responsible for the second harmonic generation, and the third-order harmonic generation, respectively.

2.2 Nonlinear Refraction (Optical Kerr Effect)

The optical Kerr effect (i.e. nonlinear refraction index) results from the third order nonlinear susceptibility $\chi^{(3)}$, which is a fourth rank tensor.

An optical wave is a real quantity and usually expressed as

$$\vec{E}(t) = \mathrm{Re}\left\{\vec{E} \exp j(\vec{k} \cdot \vec{r} + \omega t)\right\} \tag{2.3}$$

or similarly as

$$\vec{E}(t) = \frac{1}{2}\vec{E} \exp j(\vec{k} \cdot \vec{r} + \omega t) + c.c. \tag{2.4}$$

where c.c. represents the complex conjugate of the preceding term. Thus, an x-polarized optical wave, propagating in the z-direction in an isotropic medium, is represented mathematically as

$$\vec{E}(t) = \frac{1}{2}E_x \hat{x} \exp j(kz + \omega t) + c.c. \tag{2.5}$$

The third order polarization (mediated by $\chi^{(3)}$) in a material leads to a nonlinear intensity dependent contribution to its refractive index; i.e., the refractive index of the material changes as the incident intensity on the material changes. The susceptibility tensors in isotropic material can be further simplified as $\chi^{(2)} = 0$, due to inversion symmetry; the third order nonlinear

susceptibility will only have one contributing term χ_{xxxx} since the light is x-polarized and there are no means for sourcing additional polarization components.

The linear and nonlinear induced polarizations are

$$P_L = \varepsilon_0(1+\chi^{(1)})E \tag{2.6}$$

and

$$\begin{aligned} P_{NL} &= P^{(3)} \\ &= \varepsilon_0\chi_{xxxx}(\omega;-\omega,\omega,\omega)E^*EE \\ &\quad + \varepsilon_0\chi_{xxxx}(\omega;\omega,-\omega,\omega)EE^*E \\ &\quad + \varepsilon_0\chi_{xxxx}(\omega;\omega,\omega,-\omega)EEE^* \\ &= 3\varepsilon_0\chi_{xxxx}|E|^2E \\ &= \frac{3}{4}\varepsilon_0\chi_{xxxx}|E_x|^2E \end{aligned} \tag{2.7}$$

respectively. Hence,

$$P = P_L + P_{NL} = \varepsilon_0\left(1+\chi^{(1)}+\frac{3}{4}\varepsilon_0\chi_{xxxx}|E_x|^2\right)E \tag{2.8}$$

The total dielectric constant

$$\varepsilon_r^{tot} = \varepsilon_r + \Delta\varepsilon_r \tag{2.9}$$

where $\varepsilon_r = 1+\chi^{(1)} = n_o^2$ and $\Delta\varepsilon = \frac{3}{4}\chi_{xxxx}|E_x|^2$ after comparing with the expression for P.

The refractive index is related to the dielectric constant as:

$$n = \sqrt{\varepsilon_r + \Delta\varepsilon_r} \approx \sqrt{\varepsilon_r} + \frac{\Delta\varepsilon_r}{2\sqrt{\varepsilon_r}} = n_0 + \frac{3\chi_{xxxx}}{8n_0}|E_x|^2 \tag{2.10}$$

The intensity dependent refractive index for a nonlinear material is given by

$$n = n_0 + n_2|E|^2 \tag{2.11}$$

Comparing Eq.(2.10) and Eq.(2.11), the nonlinear refractive index is directly determined by the third-order susceptibility as

$$n_2 = \frac{3\chi_{xxxx}}{8n_0} = \frac{3\chi^{(3)}}{8n_0} \tag{2.12}$$

which characterizes the strength of the optical nonlinearity. The intensity I of an optical wave is proportional to $|E|^2$ as $I = \frac{1}{2\eta}|E|^2$ where η is the impedance of the medium. When comparing the optical response in the same medium, $I = |E|^2$ is taken for simplification.

2.3 Optical Chaos

Optical Chaos is observed in many nonlinear optical systems. One of the most common examples is a ring resonator. One of the most seminal works is published by Ikeda where chaotic behavior in a ring resonator was proposed and experimentally confirmed. Optical Chaos was an exciting field of research in mid-1980s and was expected at that time to lead to production of all optical devices including all optical computers. Researchers realized later the inherent limitation of the optical systems due to the non-localized nature of photons compared to highly localized nature of electrons. Research in Optical Chaos has seen a recent resurgence in the context of studying synchronization phenomena, and in developing techniques for secure optical communications. [21,23].

2.4 Optical Bistability

The phenomenon of Optical Bistability (OB) arises from a combination of the nonlinearity in the radiation-matter interaction and of a feedback mechanism [32-34]. Generally, there are two classes of OB: absorptive and dispersive OB. Absorptive OB occurs whenever the input wavelength is close to the atomic resonance of the material. An increase in the input power produces an increase in saturation, i.e., in the degree of transparency of the medium. This allows the internal field of the cavity to increase, which in return increases the saturation. Such positive feedback loop causes the switch-up process. When the input power is decreased, the internal field is intense enough to maintain the saturation. As a consequence, the transmitted power is held "ON" and one obtains a hysteresis curve. Typically, InGaAsP can be designed to have the band edge around 1.45 μm and thus can show absorptive OB when pumped at 1.55 μm. On the other hand, dispersive OB occurs whenever the input wavelength is tuned far away from the atomic resonance and hence the material is transparent. The frequency of the incident field is kept near one of the cavity frequencies, but detuned enough so that the transmission is

low. An increase in the input intensity produces an increase in the intensity of the internal field. Because the refractive index is a function of intensity, this changes the optical length of the medium in such a way that the cavity resonance is driven closer to the input frequency. In return, it increases the internal field intensity. Thus, again, we have a positive feedback loop which produces up-switching. When the incident power is decreased, the internal field is intense enough to maintain resonance between the cavity and the input frequency, and therefore one again obtains a hysteresis. An example of this phenomena is shown in Fig. 2.1 which the input wavelength is at 1.55 μm. The characteristic of bistability hysteresis can be implemented as optical switching.

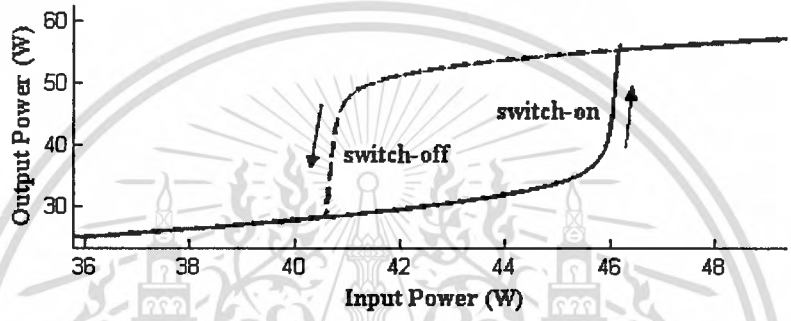

Fig. 2.1 The output power versus the input power showing the bistability hysteresis used as switch "on" and "off".

2.5 Optical Bifurcation

Bifurcation theory is the mathematical study of how and when the solution to a problem changes from there only being one possible solution to be two, which is called a bifurcation. Most commonly used in the mathematical study of dynamical systems, a bifurcation occurs when a small smooth change made to the parameter values (the bifurcation parameters) of a system causes a sudden 'qualitative' or topological change in its long-term dynamical behavior. Bifurcations occur in both continuous systems and discrete systems [35, 36].

The study of how the character of fixed points change as parameters of the system change is called bifurcation theory. (Recall that the term bifurcation is used to describe any sudden change in the dynamics of the system. When a fixed point changes character as parameter values change, the behavior of trajectories in the neighborhood of that fixed point will change. Hence the term bifurcation is appropriate here.) Being able to classify and understand the various possible bifurcations is an important part of the study of nonlinear dynamics.

2.6 Optical Soliton

How can we make beams that maintain their shape and size along propagation? As explained in the previous section, the phase between the different plane waves constructing the beam should be invariant along propagation. In a linear medium, the phase between the different plane waves depends solely on the propagation angle. It is clear then, that if all the plane wave components have the same angles; they will also have the same phase velocity and no phase difference will be acquire during propagation. If we represent the propagation direction of these plane waves by arrows, these arrows will creates a cone in space. The associated beam will propagate in this linear medium with no broadening while maintain it's shape and dimensions. This type of beams is called "Bessel beams" since their field is described by Bessel function.

In a nonlinear medium, however, each plane wave is influenced by all the others. This is because the index change is a function of the total intensity. For some nonlinearities it is possible to find an ensemble of plane waves which will delay the phase velocity of the on axis components (in comparison with the of axis components) Consequently, the phase delay between the different propagating plane waves (explained in the previous section) will be compensated by the other waves via the medium nonlinearity.

If the nonlinearity is such that the index at the beam center is higher than in the dark regions, then the plane wave that propagate on axis will experience the highest index and will propagate slower from those off axis. This high index experienced by the on axis wave can compensate for it's linear tendency to propagate faster (because it is on axis). One example in which the index of refraction fully compensates for the shorter trajectory is a hyperbolic secant solution in a Kerr type medium. The plane waves that construct the hyperbolic secant index profile (induced by the beam via the nonlinearity) have all the same phase velocity along propagation, and hence their interference (the hyperbolic secant shape) also maintains its shape and size as it propagates.

To look on solitons from the mathematical perspective. One has to find a stationary wave solution of governing nonlinear wave equation. The mathematical aspects of solitons are out of the scope of this thesis. Hence at this point, I will give just the final solution. For the exact mathematical derivation, the reader may refer to [37-39].

We start from the Maxwell equations with the following assumptions:

• The electric field in the propagation direction is negligible in comparison with the transverse electric field (paraxial approximation).

• The elecro-magnetic wave is monochromatic and its frequency is ω.

• The transverse electric field is $E(x,y,z,t) = \psi(x,y,z)exp[j(\omega t - kz)]$ where the slowly varying field $\psi(x,y,z)$ changes much slower than $\exp[j(\omega t - kz)]$

• The change in the refractive index is much smaller than 1.

For beams in Kerr-type medium (for which the index of refraction is the following function of the intensity: $n(I) = n_0 + n_2 I$, one can start from the Maxwell equations and derive the nonlinear Schrödinger equation:

$$\frac{\partial}{\partial z}\psi(x,y,z) = \left[\frac{j}{2k}\left(\frac{\partial^2}{\partial x^2} + \frac{\partial^2}{\partial y^2} + \frac{jkn_2}{n_0}|\psi(x,y,z)|^2\right)\right]\psi(x,y,z) \tag{2.13}$$

Here, z is the propagation direction, k is the wave vector, and ψ is the slowly-varying amplitude of the electric field. Among all solutions for Equation (2.13) there is one family of particular interest:

$$\psi = \sqrt{\psi_0}\,\mathrm{sec}\,h[\frac{x}{W_0}]\exp[j(\frac{z}{4z_0})] \tag{2.14}$$

Here $W_0 = \sqrt{\frac{2n_0}{n_2}}\frac{1}{k\psi_0}$ and $Z_0 = \frac{kW_0^2}{2}$. We can see that the intensity of this subfamily ($I(x,y) = |\psi|^2$) is z independent. For any chosen peak power, ψ_0, we can find a sech solution with appropriate width (the width, W_0, is a function of the peak intensity and is wider for lower peak intensities). All solutions of this sub-family (equation (2.14)) will keep their shape and size invariant along propagation. Yet, in order to observe such solitons in nature, it is not enough to have a steady state mathematical solution in hand: one should also check for the stability of this steady state solution to noise and to deviations from ideal initial condition. If the solution exemplifies a state of stationary propagation - only then it can be considered as a soliton.

2.7 Summary

This chapter introduced the fundamental concepts of different nonlinear behaviors include soliton signal which used as input for launching into micro ring resonator. Consequently, we understand of the behaviors and enable design for the nonlinear devices as mention in chapter 4 and 5. The next chapter discusses theoretical background and also detailed of enhanced nonlinearity in the both single and double ring resonators.

CHAPTER 3

MICRO RING RESONATOR CHARACTERIZATION

In applications, the penalty benefits of light traveling in micro ring resonator including the nonlinearity of light in micro ring resonator, optical switching and signal security are described as following details. Yupapin and Suchat [40] have recently reported that the nonlinear output light could be obtained after traveling along the micro ring resonator. The security of the signal can be performed by multiplexing with the chaotic signals, then the user can make the chaotic cancellation before using the require information.

In this chapter, we describe the theoretical background for this thesis. To begin, section 3.1 discusses the micro ring resonator and the material system which was used for the planar waveguide. Section 3.2 discusses the basic concept of optical add/drop filter. Section 3.3 discusses the key to analyze optical filters using Z-transforms. In the section 3.4 and 3.5 discuss enhanced nonlinearity in ring resonators.

3.1 The Micro Ring Resonator

A ring resonator is simply a waveguide shaped into a ring structure as shown in Fig. 3.1. When an input electric field, E_i, is coupled to the ring waveguide through an external bus waveguide, a positive feedback is induced and the field inside the ring resonator E_r, starts to build up. Coupling between the straight and the ring waveguide is achieved through the evanescent wave. Therefore, the gap and coupling length between them determine how much power is coupled from the straight waveguide to the ring waveguide and vice versa. The feedback mechanism is simply induced by the ring waveguide and therefore there is no need for any Bragg gratings, mirrors, or distributed feedback waveguides which are more difficult to fabricate. In such configuration, only certain wavelengths will be allowed to resonate inside the ring waveguide, thus frequency selectivity is obtained.

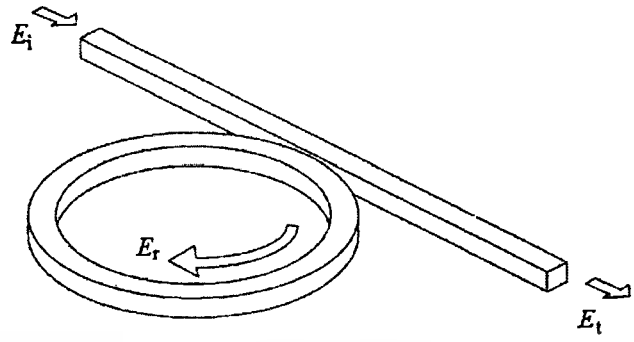

Fig. 3.1 Schematic diagram for a ring resonator coupled to a single waveguide.

The proposal to use an integrated ring resonator for a band pass filter has been made in 1969 by E. A. Marcatili [41]. The layout of the channel dropping filter is shown in Fig. 3.2. The transmission properties of the used guide consisting of a dielectric rod with rectangular cross section, surrounded by several dielectrics of smaller refractive indices have been described by E. A. Marcatili [42].

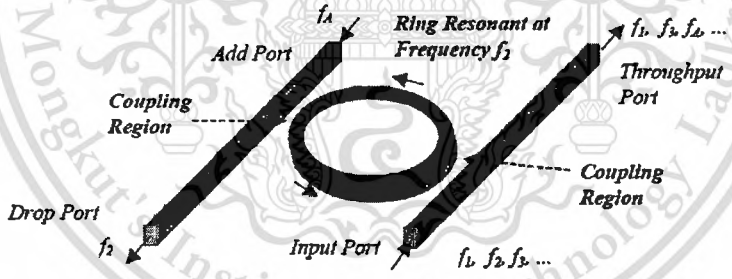

Fig. 3.2 Ring resonator channel dropping filter.

A general architecture for an autoregressive planar waveguide optical filter was demonstrated for the first time in 1996 [43]. The autoregressive lattice filters which were designed and fabricated consisted of one and two stages using Ge-doped silica waveguides.

A signal flow chart transformation for evaluating the filter transfer functions was demonstrated. Purely passive single ring resonator filters as shown in Fig. 3.2 have been realized in the material system AlGaAs-GaAs [44, 45] and Si-SiO_2 [46] and Si_3N_4- SiO_2 [47]. The radius of the used ring resonators is between 5 μm and 30 μm and the free spectral range (FSR) achieved is

between 20 nm and 30 nm. Passive ring resonators in the form of a racetrack have been realized in the material system GaInAsP [48] and AlGaAs-GaAs [49]. The filter performance is limited by bending and scattering losses in the resonator. These losses could be compensated for by using or adding an active.

3.2 Optical Add/Drop Ring Resonator Filter

A ring resonator consists of a waveguide in a closed loop. The loop can be any closed shape, such as a circle, ellipse, or racetrack. The ring is placed near one or two bus waveguides (Fig. 3.3). Typically, the input signal consists of one or more WDM channels. Signals on the input bus couple evanescently to the resonator. If a channel wavelength is resonant in the resonator, i.e., it encounters an integral multiple of 2π in phase over a round-trip, the signal intensity builds up in the ring, it couples to the output bus, and is "dropped." At the same time, a signal on the same wavelength can be added via the add port. The resonator thus functions as an add/drop multiplexer.

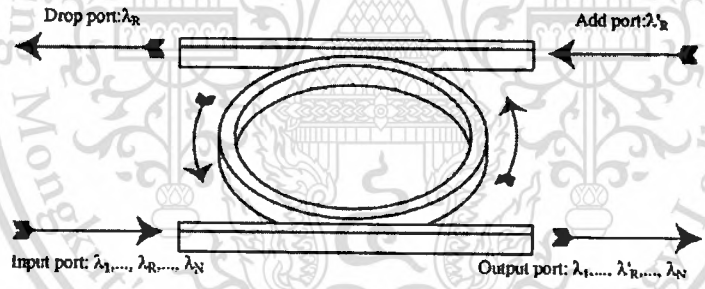

Fig. 3.3 Schematic diagram for a ring resonator coupled to two waveguides as an add/drop filter.

An incident optical signal composed of multiple wavelengths ($\lambda_1,\ldots,\lambda_R,\ldots,\lambda_N$) at the input port coupled into the ring and for a resonant wavelength (λ_R), the energy builds up in the resonator despite the small coupling and eventually the signal is coupled into the drop port. Symmetrically, a new signal at resonant wavelength (λ'_R) at the add port couples to the output port through the ring. As a result, such a configuration constitutes a very compact add/drop filter where a channel can be dropped from the WDM spectrum and replaced by a new signal on the same channel. Note that waves with a wavelength away from resonance will not repeat themselves in the ring and the coupled field interferes destructively with the wave in the resonator leading to little energy in the

resonator and little dropped power. Residual dropped power at non-resonant wavelengths is possible due to imperfections and can induce inter-band crosstalk that is detrimental to WDM applications. Moreover, if the input channel at λ_R is not completely extinguished, intra-band crosstalk. These issues will be studied and can be theoretically overcome by varying coupling parameters, inducing loss/gain in the ring and inserting additional rings between the two waveguides.

3.3 The Z-Transform Description

The filter functions arise from the interference of two or more waves that are delayed relative to each other. The incoming signal is split into multiple paths by a division of the wave front or the amplitude. Diffraction gratings are an example of wave front division, while directional couplers and partial reflectors are examples of amplitude division. After traveling along different paths, the fields are combined and interference occurs. For interference, the optical waves must have the same polarization, the same frequency and be temporally coherent over the longest delay length. When signals are recombined, their relative phases determine whether they interfere constructively or destructively. The phase Φ for each path is the product of the distance traveled, L and the propagation constant, β i.e., $\Phi = \beta L$ where $\beta = 2\pi n_e / \lambda$, which is expressed in terms of the refractive index n for a diffraction-based delay line or an effective index n_e for a waveguide delay line [50].

The individual optical path lengths are typically integer multiples of the smallest path length difference. The unit delay is defined as $T = L_u n / c$ where L_u is the smallest path length and is called the unit delay length. The refractive index is assumed to be independent of wavelength. The key to analyzing optical filters using Z-transforms is that each delay be an integer multiple of a unit delay length L_u. The phase for each path is then expressed as a multiple of βL_u, so $\Phi_p = p\beta L_u$, where p is an integer. The total transverse electric field for N paths is the sum over each optical path length given by

$$E_{out} = E_o e^{-j\Phi_0} + E_1 e^{-j\Phi_1} + E_2 e^{-j\Phi_2} + \ldots + E_{N-1} e^{-j\Phi_{N-1}}. \qquad (3.1)$$

To obtain a Z-transform of E_{out}, we express the phase as a multiple of the unit delay T. Using $\Omega = 2\pi\nu$ where $c = \nu\lambda$

$$\beta L_u = \frac{2\pi n L_u}{\lambda} = \frac{2\pi \nu n L_u}{c} = \frac{\Omega L_u n}{c} = \Omega T .$$

This gives $\Phi_p = p\beta L_u = p\Omega T$. Therefore Eq. 3.1 becomes,

$$E_{out} = E_o e^{-j0} + E_1 e^{-j\Omega T} + E_2 e^{-j2\Omega T} + \ldots + E_{N-1} e^{-j(N-1)\Omega T} . \tag{3.2}$$

For a dispersion-less line, unit delay T is a constant and using $z = e^{j\Omega T}$ in Eq. 3.2, we get

$$E_{out} = E_o + E_1 z^{-1} + E_2 z^{-2} + \ldots + E_{N-1} z^{-(N-1)} . \tag{3.3}$$

Because the delays are discrete multiples of the unit delay, the frequency response is periodic. One period is defined as the Free Spectral Range (FSR) and is given by $FSR = 1/T$. The normalized frequency $f = \omega / 2\pi$ is related to the optical frequency by $f = (\nu - \nu_c)T$ or $f = (\Omega - \Omega_c)T / 2\pi$. The center frequency $\nu_c = c / \lambda_c$ is defined so that the product of refractive index and unit length is equal to an integer number of center wavelengths, i.e., $m\lambda_c = nL_u$ where m is an integer. Propagation loss of a delay line is accounted for by multiplying z^{-1} by $x = e^{-\alpha L/2}$ where α is the average loss per unit length and L is the delay path length.

For a more realistic case for a delay line with dispersion, the FSR is given as:

$$FSR = 1/T = \frac{c}{n_g L_u}, \tag{3.4}$$

where $n_g = n_{eff} + f_o \left(dn_{eff} / df\right)_{f_o} = n_{eff} + \lambda_o \left(dn_{eff} / d\lambda\right)_{\lambda_o}$ is called as the *group refractive index* evaluated at either center frequency f_o or center wavelength λ_o.

The optical circuits are assumed to be linear and time invariant. They can be analyzed with Z-transforms using waveguide delays and directional couplers for splitting and combining signals. A schematic diagram of a directional coupler is shown in Fig. 3.4. The lines in the figure indicate waveguides of finite width and height. Two waveguides are brought close together so that their evanescent fields overlap. A power coupling ratio κ is associated with each directional coupler. For

an input on one port, the power coupled to the cross-port is κ times the input power. The length of the region where the waveguides are coupled determines the coupling ratio. The input output relation can be expressed using a 2x2 transfer matrix $\Phi_{cplr}(\kappa)$ as shown in Eq. 3.5, where κ is the power coupling ratio, and E_n^i and E_n^o, for n = 1, 2 represent the coupler input and output fields respectively.

The coupling ratio is assumed to be wavelength independent and hence the matrix elements are constants. The through and the cross-port transmission terms are given by $c = \cos\theta = \sqrt{(1-\gamma)(1-\kappa)}$ and $-js = -j\sin\theta = -j\sqrt{(1-\gamma)\kappa}$, respectively, where γ is the coupling loss and θ is equal to the coupling strength integrated over the coupling length. A complex number $-j$ represents a $-(\pi/2)$ phase shift for the cross coupled light fields.

$$\begin{bmatrix} E_1^o \\ E_2^o \end{bmatrix} = \Phi_{cplr}(\kappa)\begin{bmatrix} E_1^i \\ E_2^i \end{bmatrix}, \quad \Phi_{cplr}(\kappa) = \begin{bmatrix} c & -js \\ -js & c \end{bmatrix}. \tag{3.5}$$

Fig. 3.4 Directional coupler and I/O relations.

The basic filter structures require at least two paths for interference. The output is then the sum of each optical path. The transfer function from any input port to any output port can be written by inspection using the transmission of each path segment. The directional coupler transmission is given by $-js$ for the cross port and c for the through port. The transmission for each delay path is expressed in terms of the unit delay. A filter's transmission is then written by summing all paths between a particular input and output port.

3.3.1 Single Coupler Ring Resonator Filter (SCRR)

A ring resonator is simply a waveguide shaped into a ring structure as shown in Fig. 3.5. To determine optical filter transfer function in Z-domain, the requirements of optical filters are considered to be satisfied are:

1) Linearity of all optical components.

2) Time invariance of all optical components.

3) Optical components must be lumped (i.e. not distributed).

The effects such as backscatter of light along the length of an optical fiber or waveguide, or saturation of an optical amplifier are therefore not considered here (the former is a distributed phenomenon; the latter is a nonlinear effect).

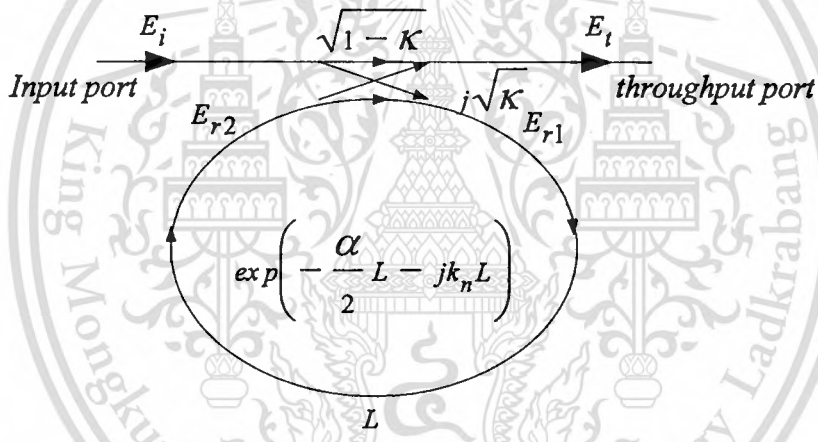

Fig. 3.5 Schematic diagram for SCRR filter.

The transfer function of this configuration is derived using Z-transform analysis. The circumference of the ring is L ($L = 2\pi R$, the radius is R), the coupling coefficient of the coupler is κ. The Z-transform parameter is represented by $z^{-1} = \exp^{-jk_nL}$ where $k_n = \frac{2\pi}{\lambda} n_{eff}$ is the propagation constant and n_{eff} is the effective index of the waveguide. The one round trip loss is $a = \exp^{-\alpha L/2}$, α is the intensity attenuation coefficient inside the waveguide [unit $length^{-1}$]. The transmitted or throughput field at the output of the straight waveguide, E_t and inserted electric field, E_i relations can be derived as followed:

$$E_t = (1-\gamma)^{1/2} \times \left[E_i \cdot \sqrt{1-\kappa} + j \cdot E_{r2} \sqrt{\kappa} \right]. \tag{3.6}$$

$$E_{r1} = (1-\gamma)^{1/2} \times \left[j \cdot E_i \cdot \sqrt{\kappa} + E_{r2} \cdot \sqrt{1-\kappa} \right]. \tag{3.7}$$

$$E_{r2} = E_{r1} \cdot a\, z^{-1}. \tag{3.8}$$

Using three equations E_t / E_i can be calculated:

$$\frac{E_t}{E_i} = (1-\gamma)^{1/2} \times \left[\frac{\sqrt{1-\kappa} - (1-\gamma)^{1/2} \cdot a z^{-1}}{1-(1-\gamma)^{1/2} \cdot \sqrt{1-\kappa} \cdot a z^{-1}} \right]. \tag{3.9}$$

The transfer function in Eq. (3.9) indicates that a ring resonator is very similar to a Fabry-Perot cavity. In the particular case shown in Fig. 3.5, the corresponding Fabry-Perot cavity would have an input mirror with a field reflectivity and a fully reflecting output mirror. However, the field propagating inside the ring cavity is a traveling wave in contrast to the Fabry-Perot cavity which resonates a standing wave.

In the following, new parameter will be used for simplification:

$$\begin{aligned} D &= (1-\gamma)^{1/2} \\ x &= D \cdot \exp^{-\alpha L/2} \\ c &= \sqrt{1-\kappa} \\ \phi &= k_n \cdot L \end{aligned} \tag{3.10}$$

The intensity relation for the output port is given by:

$$T = \frac{I_t}{I_i}(\phi) = \left| \frac{E_t}{E_i} \right|^2 = D^2 \cdot \left[1 - \frac{\left(1-x^2\right) \cdot \left(1-c^2\right)}{(1-x \cdot c)^2 + 4 \cdot x \cdot c \cdot \sin^2\left(\frac{\phi}{2}\right)} \right] \tag{3.11}$$

3.3.2 Double Coupler Ring Resonator Filter (DCRR)

Consider the architectures of double coupler ring resonator which sometime called add/drop filters as illustrated in Fig. 3.6, which are constructed by 2×2 optical couplers.

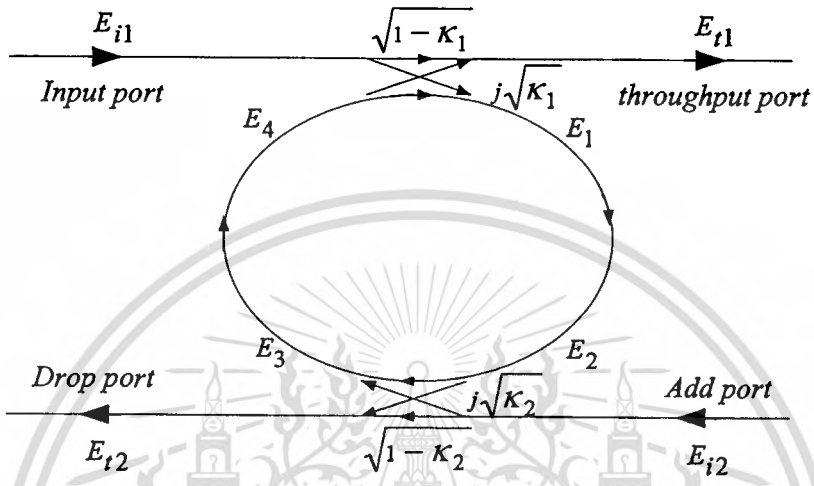

Fig. 3.6 The architecture of DCRR or add/drop filter.

Similarly, the optical transfer functions of the ring resonator filters at the throughput port and drop port for an input port E_{i1} can be derived as followed. For the first coupler (κ_1), we have

$$E_{t1} = \sqrt{1-\gamma_1}\left[j\sqrt{\kappa_1}E_4 + \sqrt{1-\kappa_1}E_{i1} \right] \tag{3.12}$$

$$E_1 = \sqrt{1-\gamma_1}\left[j\sqrt{\kappa_1}E_{i1} + \sqrt{1-\kappa_1}E_4 \right] \tag{3.13}$$

where γ and κ_1 are the loss and the coupling coefficients, respectively. The incoming light of E_{i1} and E_4 are coupled through the first coupler to the output light E_{t1} and E_1 and the output light E_1 is transmitted through the ring becomes output light E_2. According to light transmission theory in linear optical systems, we obtain the following relation between E_1 and E_2

$$E_2 = E_1 e^{-\frac{\alpha L}{2}\frac{}{2} - jk_n\frac{L}{2}} \tag{3.14}$$

where the transmission line length is $\frac{L}{2}$. The second coupler (κ_2) have the following relations:

$$E_{t2} = E_1 e^{-\frac{\alpha}{2}\frac{L}{2} - jk_n\frac{L}{2}} \cdot j\sqrt{1-\gamma_2}\sqrt{\kappa_2} \qquad \text{at } E_{i2} = 0 \tag{3.15}$$

$$E_3 = E_1 e^{-\frac{\alpha}{2}\frac{L}{2} - jk_n\frac{L}{2}}\sqrt{1-\gamma_2}\sqrt{1-\kappa_2} \tag{3.16}$$

Using the transmission theory, we obtain E_4 in terms of E_3

$$E_4 = E_3 e^{-\frac{\alpha}{2}\frac{L}{2} - jk_n\frac{L}{2}} \tag{3.17}$$

$$E_1 = \frac{E_{i1} j\sqrt{1-\gamma_1}\sqrt{\kappa_1}}{1-\sqrt{1-\gamma_1}\sqrt{1-\kappa_1}\sqrt{1-\gamma_2}\sqrt{1-\kappa_2}e^{-\frac{\alpha}{2}L - jk_nL}} \tag{3.18}$$

$$E_4 = \frac{E_{i1} j\sqrt{1-\gamma_1}\sqrt{\kappa_1}}{1-\sqrt{1-\gamma_1}\sqrt{1-\kappa_1}\sqrt{1-\gamma_2}\sqrt{1-\kappa_2}e^{-\frac{\alpha}{2}L - jk_nL}}\sqrt{1-\gamma_2}\sqrt{1-\kappa_2}e^{-\frac{\alpha}{2}L - jk_nL} \tag{3.19}$$

By using the upper equations, the transfer function for throughput port and drop port in Fig. 3.6 can thus be expressed as

Throughput port:

$$\begin{aligned}\frac{E_{t1}}{E_{i1}} &= \frac{-(1-\gamma_1)\kappa_1\sqrt{1-\kappa_2}e^{-\frac{\alpha}{2}L - jk_nL} + \sqrt{1-\gamma_1}\sqrt{1-\kappa_1}}{1-\sqrt{1-\gamma_1}\sqrt{1-\kappa_1}\sqrt{1-\gamma_2}\sqrt{1-\kappa_2}e^{-\frac{\alpha}{2}L - jk_nL}} \\ &= \frac{-(1-\gamma_1)(1-\kappa_1)\sqrt{1-\gamma_2}\sqrt{1-\kappa_2}e^{-\frac{\alpha}{2}L - jk_nL}}{1-\sqrt{1-\gamma_1}\sqrt{1-\kappa_1}\sqrt{1-\gamma_2}\sqrt{1-\kappa_2}e^{-\frac{\alpha}{2}L - jk_nL}} \\ &= \frac{-\sqrt{1-\gamma_2}\sqrt{1-\kappa_2}e^{-\frac{\alpha}{2}L - jk_nL} + \sqrt{1-\gamma_1}\sqrt{1-\kappa_1}}{1-\sqrt{1-\gamma_1}\sqrt{1-\kappa_1}\sqrt{1-\gamma_2}\sqrt{1-\kappa_2}e^{-\frac{\alpha}{2}L - jk_nL}}\end{aligned} \tag{3.20}$$

Drop port:

$$\frac{E_{t2}}{E_{i1}} = \frac{-\sqrt{1-\gamma_1}\sqrt{1-\gamma_2}\sqrt{\kappa_1 \cdot \kappa_2}\, e^{-\frac{\alpha L}{2\,2} - jk_n\frac{L}{2}}}{1-\sqrt{1-\gamma_1}\sqrt{1-\kappa_1}\sqrt{1-\gamma_2}\sqrt{1-\kappa_2}\, e^{-\frac{\alpha}{2}L - jk_nL}} \tag{3.21}$$

The intensity relations for the throughput and drop port can be obtained by normalizing the transfer functions in Eqs. (3.20) and (3.21) which are given by

$$\frac{I_{t1}}{I_{i1}} = \left|\frac{E_{t1}}{E_{i1}}\right|^2 = \frac{\begin{array}{c}1-(1-\gamma_1)\kappa_1 - 2\sqrt{1-\gamma_1}\sqrt{1-\kappa_1}\cdot\sqrt{1-\gamma_2}\sqrt{1-\kappa_2}\, e^{-\frac{\alpha}{2}L}\cos(k_nL) \\ +(1-\gamma_2)(1-\kappa_2)e^{-\alpha L}\end{array}}{\begin{array}{c}1+(1-\gamma_1)(1-\kappa_1)\cdot(1-\gamma_2)(1-\kappa_2)e^{-\alpha L} \\ -2\sqrt{1-\gamma_1}\sqrt{1-\kappa_1}\cdot\sqrt{1-\gamma_2}\sqrt{1-\kappa_2}\, e^{-\frac{\alpha}{2}L}\cos(k_nL)\end{array}} \tag{3.22}$$

$$\frac{I_{t2}}{I_{i1}} = \left|\frac{E_{t2}}{E_{i1}}\right|^2 = \frac{(1-\gamma_1)(1-\gamma_2)\cdot\kappa_1\kappa_2 e^{-\frac{\alpha}{2}L}}{\begin{array}{c}1+(1-\gamma_1)(1-\kappa_1)\cdot(1-\gamma_2)(1-\kappa_2)e^{-\alpha L} \\ -2\sqrt{1-\gamma_1}\sqrt{1-\kappa_1}\cdot\sqrt{1-\gamma_2}\sqrt{1-\kappa_2}\, e^{-\frac{\alpha}{2}L}\cos(k_nL)\end{array}} \tag{3.23}$$

For simplification, the calculation of the intensity relation does not take into account coupling losses ($\gamma = 0$) and the following parameters:

$$\begin{aligned} x &= exp\left(-\frac{\alpha}{2}L\right) \\ c_1 &= \sqrt{1-\kappa_1} \\ c_2 &= \sqrt{1-\kappa_2} \end{aligned} \tag{3.24}$$

The intensity relations Eqs. (3.22) and (3.23) are then given by

$$\frac{I_{t1}}{I_{i1}}(\phi) = \left|\frac{E_{t1}}{E_{i1}}\right|^2 = 1 - \frac{\left(1-c_1^2\right)\cdot\left(1-c_2^2x^2\right)}{\left(1-c_1c_2x\right)^2 + 4c_1c_2x\sin^2\left(\frac{\phi}{2}\right)} \tag{3.25}$$

$$\frac{I_{t2}}{I_{i1}}(\phi)=\left|\frac{E_{t2}}{E_{i1}}\right|^2=\frac{\left(1-c_1^2\right)\cdot\left(1-c_2^2\right)\cdot x}{\left(1-c_1c_2x\right)^2+4c_1c_2xsin^2\left(\frac{\phi}{2}\right)} \tag{3.26}$$

3.4 Enhanced Nonlinearity in Single Ring Resonator

In section 3.4 and 3.5, we will carefully study such enhancement and its projection on the dynamic performance of the micro ring resonator for all-optical switching applications. We will concentrate on the reduction achievable in the switching power of a micro ring due to the resonant condition.

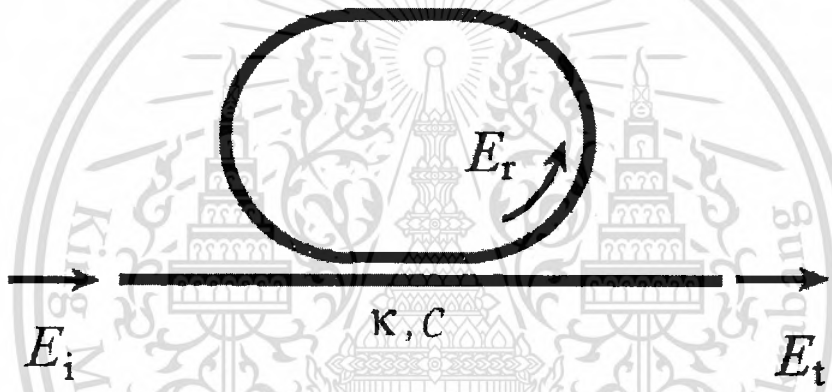

Fig. 3.7 The waveguide layout of SCRR.

For a small range of detuning, i.e., much smaller than the 3-dB bandwidth of the micro ring resonance, a small signal analysis approach is enough to understand the dynamic behavior of the resonator and to determine its switching enhancement. In such analysis, we will assume that the linear parameters of the micro ring resonator are constants with respect to time. Without loss of generality, we will consider the SCRR filter case in Fig. 3.7 that we have introduced in section 3.3.1. At steady state, the field transmittance of the filter is given by

$$\frac{E_t}{E_i}=\frac{c-a\,e^{j\phi_0}}{1-ca\,e^{j\phi_0}}. \tag{3.27}$$

where $a=\exp(-\alpha L/2)$ is the round trip field attenuation of the microring, c is the field transmittance coefficient, and $\phi_0=\beta L$ is linear phase shift in the ring. β is the wave propagation

constant associated with the fundamental mode supported by the ring waveguide, and L is the circumference of the ring. One useful feature of a ring resonator is that the original power gets to build up in the ring and keeps circulating inside the ring. The buildup factor B, which is defined as the ratio of the power circulating inside the ring to the input power, is given by [51]

$$B = \frac{P_r}{P_i} = \frac{1-c^2}{1+c^2a^2-2ca\cos\phi_0} \tag{3.28}$$

where P_i is the input power, P_r is the average power inside the ring. Under conditions that the incident light is on resonance with the ring and the loss is negligible ($a = 1$), the maximum value of the buildup factor $B_{\max} = (1+c)/(1-c)$. Thus, when c is very close to unity, the power circulating inside the fiber ring becomes very high. This power buildup can induce nonlinear effects if the ring possesses an intensity-dependent nonlinear refractive index n_2 that results from the third-order susceptibility ($\chi^{(3)}$) of the waveguide material [51]. The nonlinear refractive index n_2 can be included in the single-pass phase shift as

$$\phi = \phi_0 + \phi_{NL} \cong \beta L + \gamma L_{eff} P_r \tag{3.29}$$

where $L_{eff} = [1-\exp(-\alpha L)]/\alpha$, is the effective interaction length due to the loss and γ is the nonlinearity coefficient (related to n_2 by $\gamma = 2\pi n_2 / \lambda A_{eff}$, where λ is the input wavelength and A_{eff} is the effective core area of the waveguide). ϕ_0 and ϕ_{NL} are the single-pass linear and nonlinear phase shifts, respectively. In such a nonlinear case, ϕ_0 in Eq. (3.28) should now be replaced by ϕ. Thus, by substituting Eq. (3.29) into Eq. (3.28), we get a transcendental equation for the single-pass phase shift as

$$\phi(P_i, \phi_L) = \phi_L + \gamma L_{eff} \frac{1-c^2}{1+c^2a^2-2ca\cos\phi(P_i, \phi_L)} P_i \tag{3.30}$$

The nonlinear response of switching device can be evaluated by the derivative of phase shift ϕ with respect to input power P_i. This derivative can be expressed as

$$\frac{d\phi}{dP_r} = \frac{d\phi}{d\phi_0}\frac{d\phi_0}{dP_r}\frac{dP_r}{dP_i} \approx \frac{8Ln_2}{\pi\lambda A_{eff}} F^2 \tag{3.31}$$

where F is resonator finesse [51].

3.5 Enhanced Nonlinearity in Add/Drop Ring Resonator

The transmission equation from input port to drop port for the DCRR as shown in Fig. 3.6 is given by

$$\frac{E_{t2}}{E_{i1}} = \frac{s_1 s_2 \sqrt{\gamma} e^{j\phi_0}}{1 - c_1 c_2 \gamma e^{j\phi_0}} \tag{3.32}$$

where c_1, s_1 and c_2, s_2 are the coupling coefficients for the two couplers respectively. Critical coupling condition for the DCRR is defined to be $\left|E_{t2}/E_{i1}\right|^2 = 1$, i.e. all light goes through the drop port, which gives $s_{2c} = \sqrt{1 - c_1^2 e^{-\alpha L}}$. Since $s_{2c} = s_1$, symmetric DCRR (with two identical couplers) will operate at noncritical coupling. The phase shift of the drop port field (E_{t2}) is

$$\phi = \pi + \phi_0 + \arctan\left[\frac{c^2\gamma \sin\phi_0}{1 - c^2\gamma\cos\phi_0}\right] \tag{3.33}$$

Similar to SCRR, the nonlinear effect can be included by applying equation (3.29) to the computation of ϕ as follow.

$$\phi = \phi_0 + \frac{2\pi n_2 \frac{L}{2} P_2}{\lambda A_{eff}} + \frac{2\pi n_2 \frac{L}{2} P_4}{\lambda A_{eff}} \tag{3.34}$$

where P_2 and P_4 are circulating powers, respectively.

3.6 Summary

The main goal of this chapter suggests nonlinear enhancement in micro ring resonator and we then can get the nonlinear transfer functions which used to characterize the nonlinear behaviors such as chaos, bifurcation, and bistability. Each behavior can be implemented for design of many applications as describe in chapter 4.

CHAPTER 4

NONLINEAR DEVICE BASED MICRO RING RESONATOR

In this chapter, we design the optical devices result from nonlinear device based micro ring resonator. The results of nonlinear device design can be applied for dark-bright solitons conversion and storage and tunable light source generation.

4.1 Dark-Bright Solitons Conversion

Nonlinear behaviors have shown the potential applications in many research areas, where the interesting concept is that the penalty of nonlinearity becomes a benefit [52, 53]. They have shown that nonlinear behaviors of light within waveguide could be used to form the benefits in various research applications. To date, the progress in new linear devices technology is quite slow, which may be limit in the near future. Therefore, the trend of new devices and technology is becoming the subject of much research interest today. Nonlinear devices are one of the target devices and technologies where research should be encouraged into order to bring a new era of technology. Furthermore, through the use of nonlinear device known as "nano-ring resonator" in various applications, promising and interest results have been reported [54, 55]. Further, the evidence of the device using in the practical work has also been report [56]. The device is fabricated by using the nonlinear material called "InGaAsP/InP", where the nonlinear refractive index is one of the properties of the key phenomenon, and good result is obtained. To begin this concept, we introduce the device known as a "ring resonator", which is in a circular form or planar waveguide. Yupapin et al [57] have shown the promising applications when the ring radius is down to a micrometer or nanometer. For instance, the ultra fast switching can be easily generated by using a remarkably simple arrangement, where the achievement of the switching time of attosecond and beyond is confirmed. The most interesting results are seen when the light pulse can be slowed down, stopped and stored within the nonlinear nano-waveguide, where the results of the signal amplification within the tiny device have shown the great successfully obtained.

Dark and bright soliton behaviors have been widely investigated in different forms [58, 59]. The use of soliton, i.e. bright soliton in long distance communication link has been implemented for nearly two decades, however, the interesting works using bright solitton in communication remain, whereas the use a soliton pulse within a micro ring resonator for communication security has been studied[60]. The interesting results are when the technique could be implemented within a tiny device such as a micro ring and nano ring resonators and could be implemented within the mobile hand set [60, 61]. Dark soliton is one of the soliton properties, whereas the soliton amplitude is vanished or minimized during the propagation in media, therefore, the dark soliton detection is difficult. The investigation of dark soliton behaviors has been reported [62, 63], where one point of them has shown the interesting results, where the dark soliton can be stabilized [64] and converted into bright soliton [65] and finally detected. This means that we can use the dark soliton penalty due to the low level of the peak power to be the benefit, where the promising idea is that a dark soliton can be performed the communication transmission carrier where the recovery can be retrieved by the dark-bright soliton conversion. Actually, we are looking for the simple technique that can be employed to detect the dark soliton. Yupapin and Suwancharoen have reported [27] the interesting results of light pulse propagating within a nonlinear micro ring device, where the transfer function of the output at the resonant condition is derived and used. They found that the broad spectrum of light pulse can be transformed to the discrete pulses. Recently, Pornsuwancharoen and Yupapin [66] have reported that a soliton pulse can be localized within a nano-waveguide, where they have design a system which is consisted of micro and nano ring resonators, the soliton pulse can be stored within the nano-waveguide. In this paper, we have shown that after the clean dark soliton is input and chopped to be the noisy signals for security purpose within the nonlinear ring resonator system, which can be transmitted into the transmission link safely. The required users can retrieve the original signal via an add/drop filter, where they can chose to retrieve in either bright or dark soliton pulses. However, the device parameters are the given keys for the end users, where they can use to form the device that can be used to retrieve the signals in the link or network.

An optical soliton is recognized as a powerful laser pulse, which can be used to enlarge the optical bandwidth when propagating within the nonlinear micro ring resonator [66]. Moreover, the superposition of self-phase modulation soliton pulses can keep the large output power. Initially, the optimum energy is coupled into the waveguide by a lager effective core area device, i.e. micro ring resonator. Then the smaller one is connected to transfer the soliton power, however, the optical loss

is involved in the transferring link. The filtering characteristic of the optical signal is presented within an add/drop filter, where the suitable parameters can be controlled to obtain the required output energy. To obtain the required soliton power after propagating within the ring resonator, the suitable coupling power into the device is required, i.e. coupling coefficient (K), whereas the interference signal is a minor effect compared to the loss associated to the direct passing through.

We are looking for a stationary dark soliton pulse, which is introduced into the multi-stage micro ring resonators as shown in Fig. 4.1,

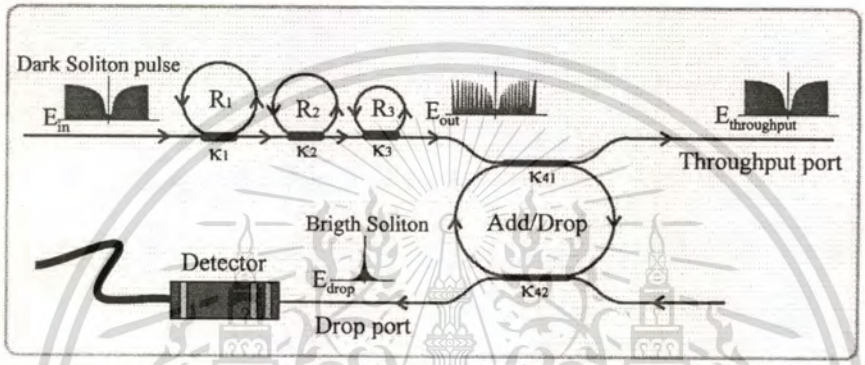

Fig. 4.1 A schematic of a dark-bright soliton conversion system, where R_s: ring radii, K_s: coupling coefficients, K_{41} and K_{42} are the add/drop coupling coefficients.

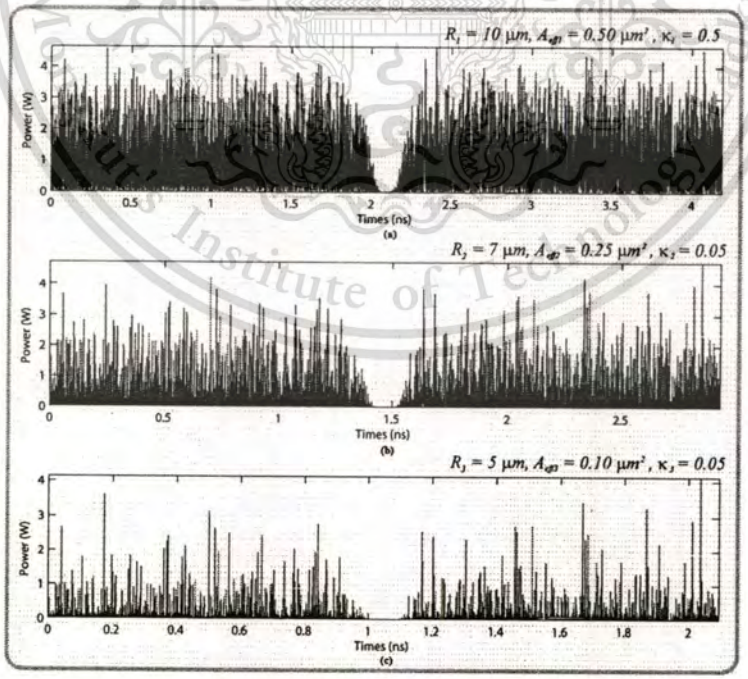

Fig. 4.2 Results of the soliton signals within the ring resonator system, where (a) in ring R_1, (b) in ring R_2 and (c) in ring R_3.

In operation, a dark soliton pulse with 50 ns pulse width, the maximum power of 1.0 W is input into the dark-bright solitons conversion system as shown in Fig. 4.1. The suitable ring parameters are used, for instance, ring radii R_1= 10.0 μm, R_2= 7.0 μm, and R_3= 5.0 μm. In order to make the system associate with the practical device [67, 68], the selected parameters of the system are fixed to λ_0 = 1.55 μm, n_0 = 3.34 (InGaAsP/InP), A_{eff} = 0.50, 0.25 μm^2 and 0.10 μm^2 for a micro ring and nano ring resonator [56], respectively, α = 0.5 $dBmm^{-1}$, γ = 0.1. The coupling coefficients (kappa, κ) of the micro ring resonator are ranged from 0.05 to 0.90. The nonlinear refractive index is n_2=2.2 x 10^{-17} m^2/W. In this case, the wave guided loss used is 0.5$dBmm^{-1}$. The input dark soliton pulse is chopped (sliced) into the smaller signals as shown in Fig. 4.2(a). Figures 4.2(b) and 4.2(c) are the output signals of the filtering signals within the rings R_2 and R_3. We find that the output signals from R_3 are smaller than from R_1, which is more difficult to detect when it is used in the link. In fact, the multi-stage ring system is proposed due to the different core effective areas of the rings in the system, where the effective areas can be transferred form 0.50 μm^2 to 0.10 μm^2 with some losses. The soliton signals in R_3 is entered in the add/drop filter, where the dark-bright solitons conversion. Results obtained when a dark soliton pulse is input into a micro and nano ring resonator system as shown in Figs. 4.3 and 4.4. The parameters used are the same as in Fig. 4.2, where the only change is the add/drop filter parameters. It is formed by two couplers and a ring radius (R_d) of 10 μm, the coupling constants (κ_{11} and κ_{12}) are the same values (0.50). When the add/drop filter is connected to the third ring (R_3), the dark-bright solitons conversion are seen. The bright soliton and dark solitons are detected by the through (throughput) and drop ports as shown in Fig. 4.1, respectively.

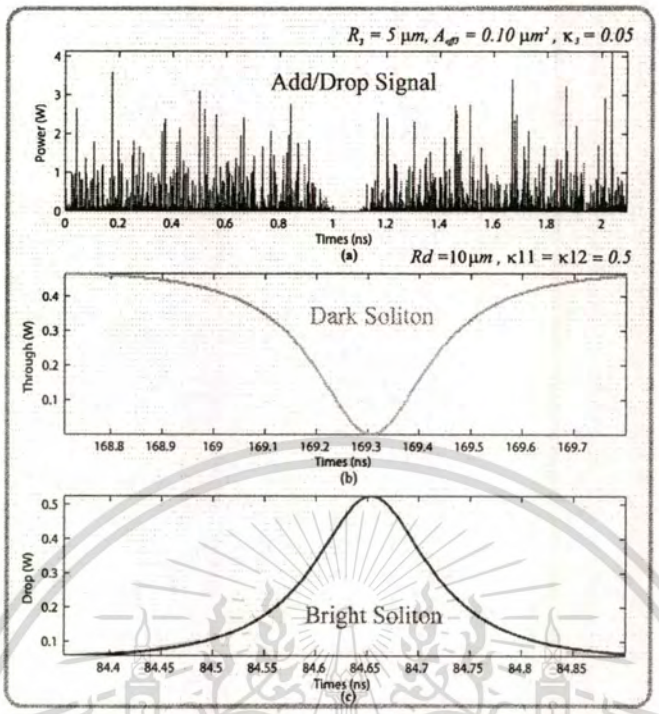

Fig. 4.3 Results of the optical solitons, where (a) the signals in R_3, (b) a dark soliton and (c) a bright soliton. the input dark soliton power is 1 W, κ_1 = 0.5, R_d = 10 μm.

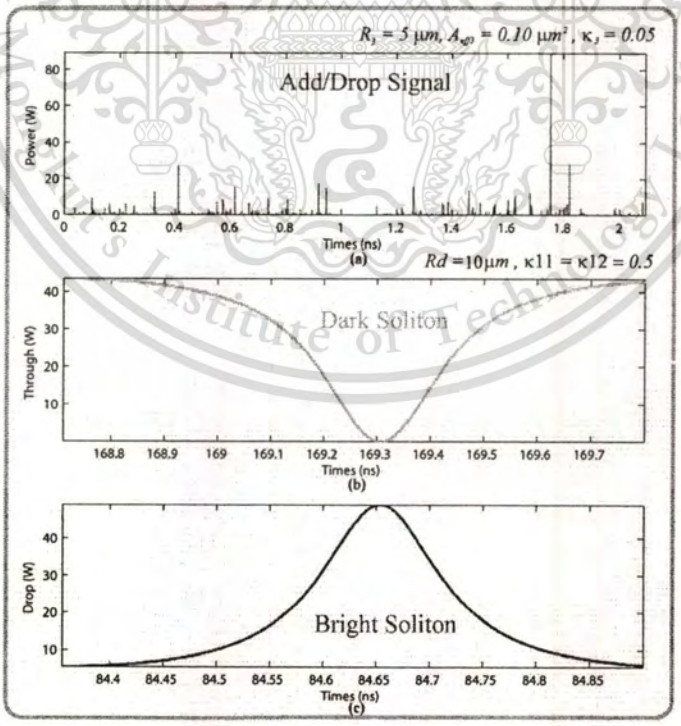

Fig. 4.4 Results of the optical solitons, where (a) the signals in R_3, (b) a dark soliton and (c) a bright soliton. the input dark soliton power is 1 W, κ_1 = 0.9, R_d = 10 μm.

Temporal and spatial solitons are the soliton characteristics, which they present the soliton waveforms between the soliton power with time and wavelength, respectively. In the signal security concept, it is proposed by using the temporal dark soliton pulse input into the micro ring resonator system, whereas the required signals can be multiplexed into the dark soliton pulse. The multiplexed signals, i.e. soliton pulse and the required signals are then chopped to be the noisy signals and transmitted into the link safely. Furthermore, the output soliton power, i.e. link power budget can be specified by the input dark soliton as shown in Figs. 4.3 and 4.4, the smaller input soliton power is applied, the smaller power budget is obtained. The required users can retrieve the original signal via the add/drop filter, where they can chose to retrieve in either bright or dark soliton pulses. However, the device parameters are the given keys for the end users, especially, the add/drop filter, where they can form the device that can be used to retrieve the signals in the link or network. The different temporal soliton response time is seen in Figs. 4.3 to 4.5, which can also be used to form the security key where the response time of 84.65 ns is noted in this work, which is designed by the add/drop filter parameters. The response time is changed when the different add/drop filters are applied. Moreover, the power budget is also important for soliton communication concept, for instance, the output power of 500 mW is obtained as shown in Fig. 4.3, which is enough to operate in the link. Where more/less output power can be desired and obtained by using the appropriate initial input soliton power and the coupling coefficient (κ_1) values as in the earlier discussion. In practice, the result obtained in Fig. 4.4 is the best signals for security purpose among the results because the signals in ring R_3 is difficult to retrieve the original signals. The other key parameter is the radius of ring R_3, whereas the nano-waveguide is required to perform the amplified signals, i.e. soliton pulse, for instance, the ring radius of 5 μm, with the effective core area A_{eff} of 0.10 μm^2 is used to obtain the nano-scale ring resonator [56].

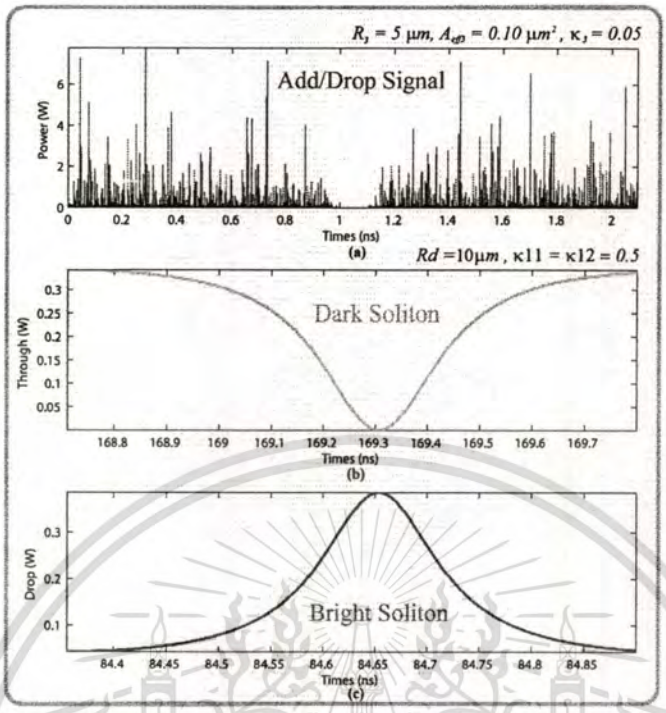

Fig. 4.5 Results of the optical solitons, where (a) the signals in R_3, (b) a dark soliton and (c) a bright soliton. the input dark soliton power is 1 W, K_1 = 0.4, R_d= 10 μm.

The dark-bright signal amplification system is as shown in Fig. 4.6. Firstly, when the bright soliton system is operated, the large bandwidth within the micro ring device can be generated by using a soliton pulse input into the nonlinear micro ring resonator. Similarly, the input soliton pulse is chopped (sliced) into a smaller signal spreading over the spectrum as shown in Fig. 4.7, which is shown that the large bandwidth signal is generated within the first ring device. A soliton pulse with 50 ns pulse width, and maximum power at 0.65 W is input into the system. The results are obtained when a bright soliton pulse is input into the ring resonator system, whereas the parameters used are R_1= 10 μm, A_{eff1} = 0.50 μm^2, R_2= 7 μm, A_{eff2} = 0.25 μm^2, R_3= 5 μm, A_{eff3} = 0.10 μm^2 and κ_1 = 0.2 and κ_2 = κ_3 = 0.05. The continuous spectra output which is 25 times larger than the input, it is obtained and seen in Fig. 4.7(c). Secondly, a soliton pulse is input into a micro ring resonator system for within NRR, where the parameters used are R_1= 10 μm, A_{eff1} = 0.50 μm^2, R_2= 7 μm, A_{eff2} = 0.25 μm^2, R_3= 5 μm, A_{eff3} = 0.10 μm^2 and κ_1 = 0.2 and κ_2 = κ_3 = 0.05.A dark soliton pulse is chopped (sliced) into the smaller signals as shown in Fig. 4.8(a). Figures 4.8(b) and 4.8(c) are the output signals of the filtering signals within the rings R_2 and R_3. Results obtained when a dark

soliton pulse is input into a micro and nano ring resonator system as shown in Figs. 4.6(b). The continuous spectra output with 25 times larger than the input is obtained and seen in Fig. 4.7(c). The coupling coefficients are given as shown in the figures.

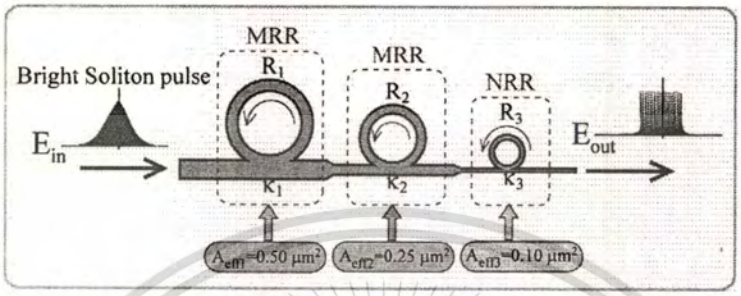

(a) Amplified bright soliton within NRR.

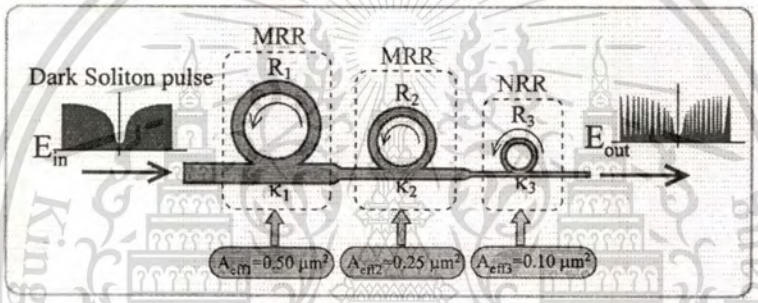

(b) Amplified dark soliton within NRR.

Fig. 4.6 A schematic of the amplified dark-bright soliton conversion system, where R_s: ring radii and K_s: coupling coefficients, where MRR: Micro ring resonator, NRR:Nano-ring resonator.

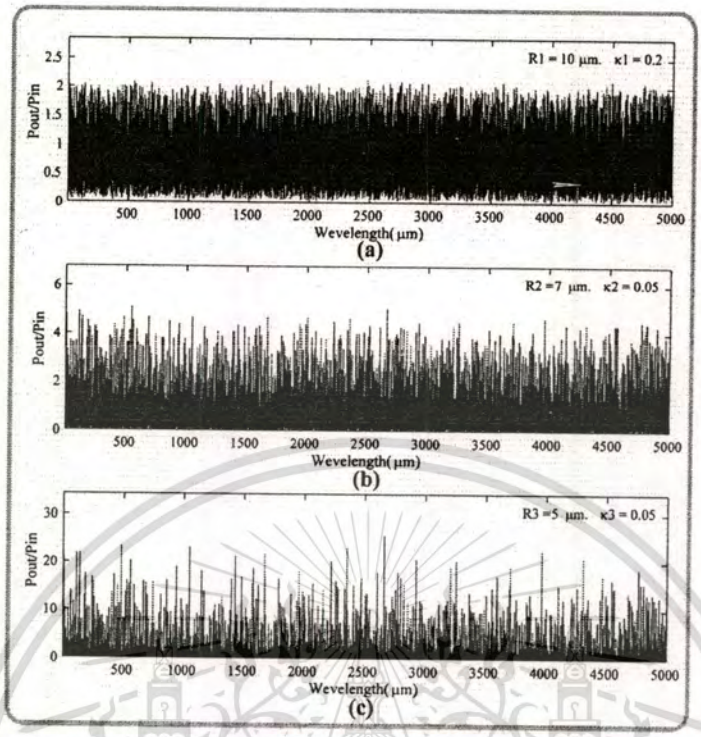

Fig. 4.7 Results obtained when a soliton pulse is input into a micro ring resonator system for within NRR.

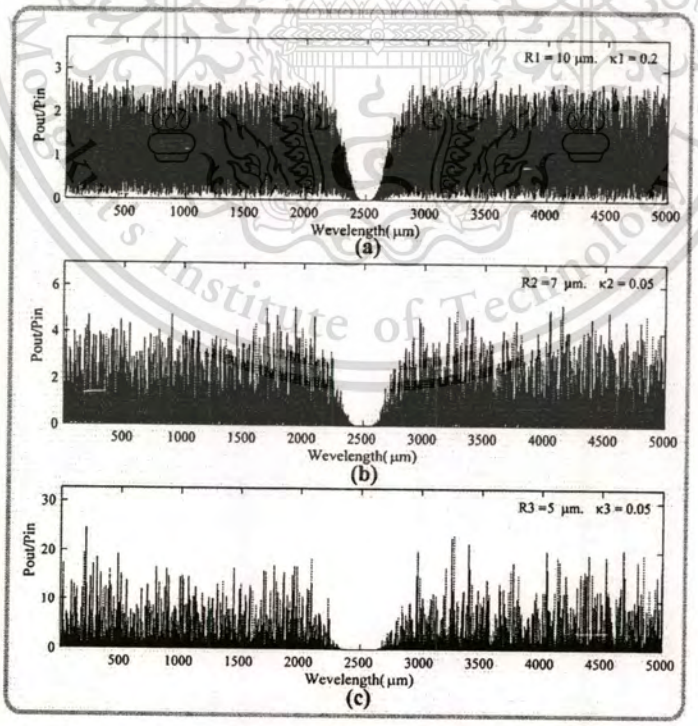

Fig. 4.8 Results obtained when a soliton pulse is input into a micro ring resonator system for within NRR.

4.2 Storage and Tunable Light Source Generation

Nonlinear device is one of the target device that should be encouraged to research for the new era of device technology. The interesting results of the use of nonlinear device have been reported recently [57, 67], they have shown the interesting and promising results of using the nonlinear device known as a "nano-ring resonator" in various applications. Furthermore, the evidence of such a device using in the laboratory has also been reported [56]. Such a device is fabricated by using the nonlinear material called "**InGaAsP/InP**", where the nonlinear refractive index value is one of the properties to obtain the good results. To begin this concept, we introduce the device known as a "ring resonator", which is in the circular form or planar waveguide, where Yupapin and Pornsuwancharoen [69] have shown that the promising application is occurred when the ring radius is down to a micrometer or nanometer scale. For instance, the ultra fast switching can be easily generated by using a remarkably simple arrangement, where the generation of the switching time of attosecond and beyond is confirmed [57]. The most interesting results is seen when light pulse can be slow down, stopped and stored within the nonlinear nano-waveguide [69], where the signal amplification within the tiny device has shown the great successful. In this work, we propose two different results that can be used to form the broadband light source and store within the tiny device. Initially, a soliton pulse with center wavelength at 1.55 μm is input into the novel system, whereas the selected pulse can be filtered, amplified and stored within the nano-waveguide. Firstly, the dense wavelength source can be formed by using the stored wavelength at 1.50 μm, and secondly, it can be regenerated by using the stored wavelength at 0.50 μm. The operation system can be used to analyze and describe the concept of broadband light source generation and regeneration, which is allowed to perform the tunable light source, whereas the light source with the specific wavelength can be selected, i.e. filtered and stored.

Initially, the optimum energy is coupled into the waveguide by a lager effective core area device, i.e. ring resonator as shown in Fig. 4.9 Then the smaller ones are connected to form the storage unit. The filtering characteristic of the optical signal is presented within a ring resonator and an add/drop filter, where the suitable parameters can be controlled to obtain the required output spectra. To maintain the soliton pulse propagating within the ring resonator, the suitable coupling power into the device is required, whereas the interference signal is a minor effect compared to the

loss associated to the direct passing through. A soliton pulse, which is introduced into the multi-stage micro ring resonators as shown in Figs. 4.9

In operation, the large bandwidth signal within the micro ring device can be generated by using a soliton pulse input into the nonlinear micro ring resonator. This means that the broadband light spectra can be generated after the soliton pulse is input into the ring resonator system. The schematic diagram of the proposed system is as shown in Fig. 4.9 A soliton pulse with 50 ns pulse width, peak power at 2 W is input into the system. The suitable ring parameters are used, for instance, ring radii R_1= 15.0 μm, R_2= 10.0 μm, R_3=R_s= 5.0 μm and R_5=R_d= 20.0 μm as shown in Fig. 4.10 In order to make the system associate with the practical device [56], the selected parameters of the system are fixed to λ_0 = 1.55 μm, n_0 = 3.34 (**InGaAsP/InP**), A_{eff} = 0.50, 0.25 μm^2 and 0.10 μm^2 for a micro ring and nano ring resonator, respectively, α = 0.5 $dBmm^{-1}$, γ = 0.1. The coupling coefficient (kappa, κ) of the micro ring resonator ranged from 0.1 to 0.96. The nonlinear refractive index is n_2=2.2 x 10^{-13} m^2/W. In this case, the wave guided loss used is 0.5$dBmm^{-1}$. The input soliton pulse is chopped (sliced) into the smaller signals spreading over the spectrum as shown in Figs. 4.10(b) and 4.11(b), which is shown that the large bandwidth signal is generated within the first ring device. The biggest output amplification is obtained within the nano-waveguides (rings R_3 and R_4) as shown in Figs. 4.10(d), 4.10(e), 4.10(f), 4.11(d), 4.11(e) and 4.11(f), whereas the maximum power of 10 W is obtained at the center wavelength of 1.50 and 0.50 μm, respectively. The coupling coefficients are given as shown in the figures. The coupling loss is included due to the different core effective areas between micro and nano ring devices, which is given by 0.1dB.

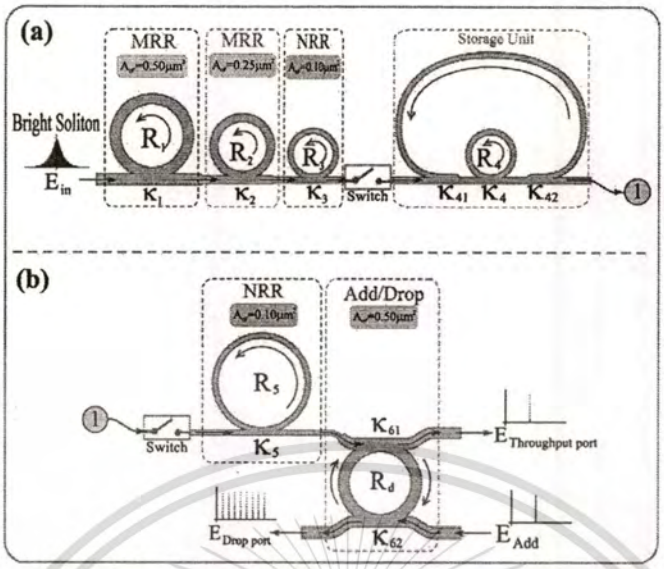

Fig. 4.9 A storage and tunable light source generation system, where R_s: ring radii, κ_s: coupling coefficients, κ_{41} κ_{42}: coupling losses κ_{61} and κ_{61} are the add/drop coupling coefficients.

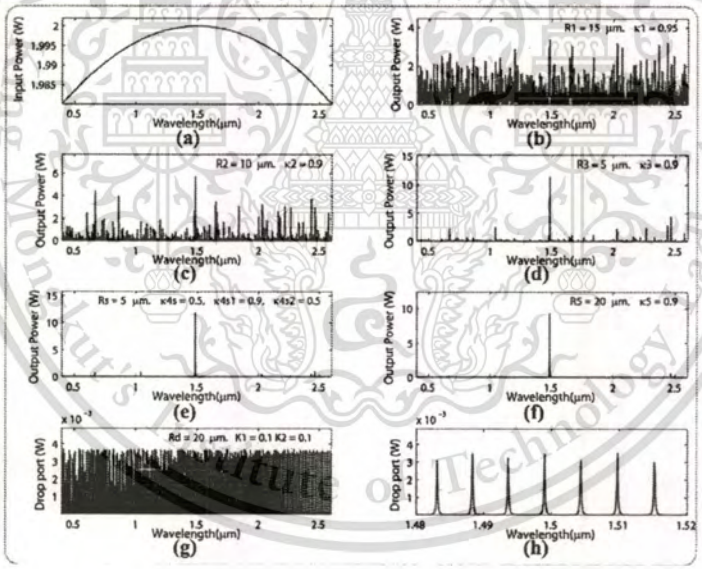

Fig. 4.10 Results obtained with the storage wavelength at 1.50 μm, where (a) input soliton, (b) ring R_1, (c) ring R_2, (d) ring R_3, (e) storage ring (R_s), (f) ring R_5, (g) and (h) drop port signals.

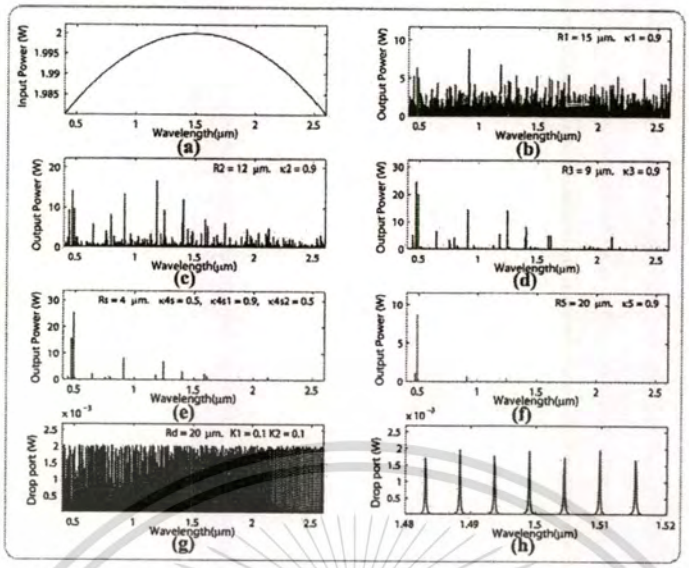

Fig. 4.11. Results obtained with the storage wavelength at 0.50 μm, where (a) input soliton, (b) ring R_1 and (c) ring R_2, (d) ring R_3, (e) storage ring (R_s), (f) ring R_5, (g) and (h) drop port signals.

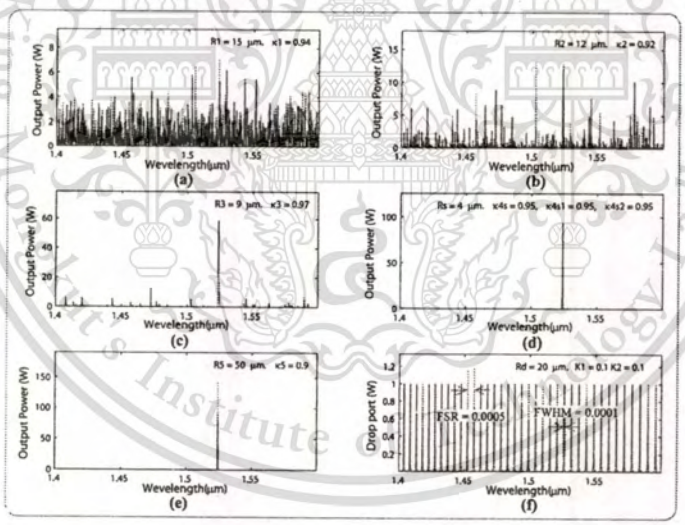

Fig. 4.12. Results obtained with the storage wavelength at 1.52 μm, where (a) ring R_1 and (b) ring R_2, (c) ring R_3, (d) storage ring R_s, (e) ring R_5 and (f) drop port signals.

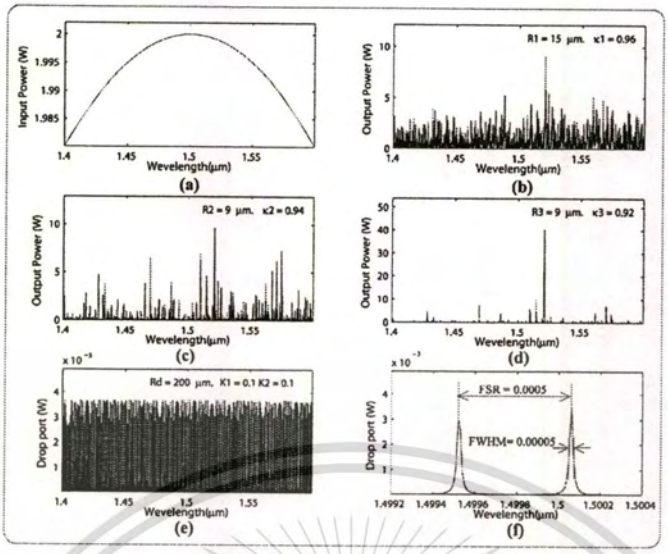

Fig. 4.13 Results obtained with the storage wavelength at 1.50 μm, where (a) input soliton, (b) ring R_1 (c) ring R_2, (d) ring R_3, (e) and (f) drop port signals.

CHAPTER 5

DNA CODE AND HIGH SECURITY PACKET SWITCHING

In this chapter, we propose DNA encoding of nonlinear signals in nonlinear micro ring resonator. The generated nonlinear signals can be formed as the logical pulses "A" or "T" or "C" or "G" using the signal quantizing method. And, we propose a new system of the high secured packet switching using the nonlinear behaviors of soliton in a micro ring resonator. Results obtained have shown the potential of using such a proposed device, in which the packet switching data can be performed and secured.

5.1 DNA Codes Generation

Light from a monochromatic light source is launched into a ring resonator with constant light field amplitude (E_0) and random phase modulation ($ø_0$) as shown in Fig. 5.1, which is the combination of terms in attenuation (α) and phase(f_0) constants, which results in temporal coherence degradation. Hence, the time dependent input light field (E_{in}), without pumping term, can be expressed as [70]

$$E_{in}(t) = E_0 \exp^{-\alpha L + j\phi_0(t)}. \tag{5.1}$$

where L is a propagation distance (waveguide length). We assume that the nonlinearity of the optical ring resonator is of the Kerr-type, i.e., the refractive index is given by

$$n = n_0 + n_2 I = n_0 + (\frac{n_2}{A_{eff}})P, \tag{5.2}$$

where n_0 and n_2 are the linear and nonlinear refractive indexes, respectively. I and P are the optical intensity and optical power, respectively. The effective mode core area of the device is given by A_{eff}. For the microring and nanoring resonators, the effective mode core areas range from 0.10 to 0.50 μm^2 [68,56]

When a Gaussian pulse is input and propagated within a ring resonator, the resonant output is formed, thus, the normalized output of the light field is the ratio between the output and input fields ($E_{out}(t)$ and $E_{in}(t)$) in each roundtrip, which can be expressed as [71]

$$\left|\frac{E_{out}(t)}{E_{in}(t)}\right|^2 = (1-\gamma)\left[1-\frac{(1-(1-\gamma)x^2)\kappa}{(1-x\sqrt{1-\gamma}\sqrt{1-\kappa})^2+4x\sqrt{1-\gamma}\sqrt{1-\kappa}\sin^2(\frac{\phi}{2})}\right] \tag{5.3}$$

Equation (5.3) indicates that a ring resonator in the particular case is very similar to a Fabry-Perot cavity, which has an input and output mirror with a field reflectivity, (1-κ), and a fully reflecting mirror. k is the coupling coefficient, and $x = \exp(-\alpha L/2)$ represents a roundtrip loss coefficient, $\phi_0 = kLn_0$ and $\phi_{NL} = kL(\frac{n_2}{A_{eff}})P$ are the linear and nonlinear phase shifts, $k = 2\pi/\lambda$ is the wave propagation number in a vacuum. Where L and α are a waveguide length and linear absorption coefficient, respectively. In this work, the iterative method is introduced to obtain the results as shown in equation (5.3), similarly, when the output field is connected and input into the other ring resonators.

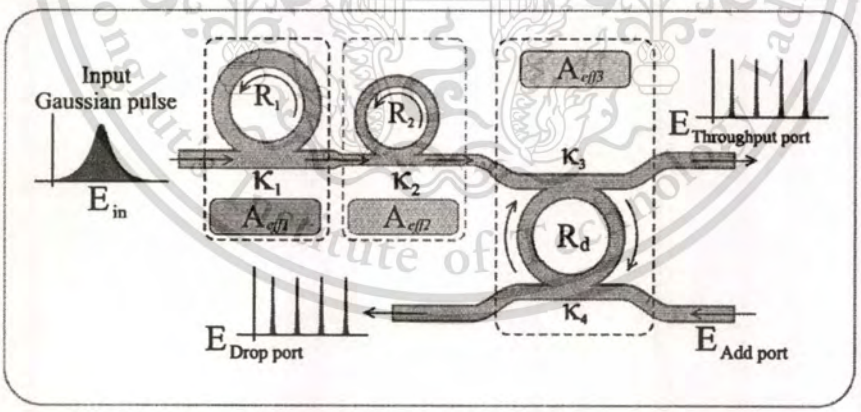

Fig. 5.1 A schematic of a Gaussian soliton generation system, where R_s: ring radii, κ_s: coupling coefficients, R_d: an add/drop ring radius, A_{eff}s: Effective areas.

The input optical field as shown in equation (5.1), i.e. a Gaussian pulse, is input into a nonlinear micro ring resonator. By using the appropriate parameters, the chaotic signal is obtained by using equation (5.3). To retrieve the signals from the chaotic noise, we propose to use the add/drop

device with the appropriate parameters. This is given in details as followings. The optical outputs of a ring resonator add/drop filter can be given by the equations (5.4) and (5.5) [71].

$$\left|\frac{E_t}{E_{in}}\right|^2 = \frac{(1-\kappa_1)-2\sqrt{1-\kappa_1}\cdot\sqrt{1-\kappa_2}e^{-\frac{\alpha}{2}L}\cos(k_nL)+(1-\kappa_2)e^{-\alpha L}}{1+(1-\kappa_1)(1-\kappa_2)e^{-\alpha L}-2\sqrt{1-\kappa_1}\cdot\sqrt{1-\kappa_2}e^{-\frac{\alpha}{2}L}\cos(k_nL)} \quad (5.4)$$

And

$$\left|\frac{E_d}{E_{in}}\right|^2 = \frac{\kappa_1\kappa_2 e^{-\frac{\alpha}{2}L}}{1+(1-\kappa_1)(1-\kappa_2)e^{-\alpha L}-2\sqrt{1-\kappa_1}\cdot\sqrt{1-\kappa_2}e^{-\frac{\alpha}{2}L}\cos(k_nL)} \quad (5.5)$$

where E_t and E_d represent the optical fields of the throughput and drop ports respectively. Where $\beta = kn_{eff}$ represents the propagation constant, n_{eff} is the effective refractive index of the waveguide, and the circumference of the ring is $L = 2\pi R$, here R is the radius of the ring. In the following, new parameters will be used for simplification, where $\phi = \beta L$ is the phase constant. The chaotic noise cancellation can be managed by using the specific parameters of the add/drop device, which the required signals at the specific wavelength band can be filtered and retrieved. $\kappa_1$and κ_2 are coupling coefficient of add/drop filters, $k_n = 2\pi/\lambda$ is the wave propagation number for in a vacuum, and the waveguide (ring resonator) loss is α = 0.5 dBmm^{-1}. The fractional coupler intensity loss is γ = 0.1. In the case of add/drop device, the nonlinear refractive index is neglected.

The schematic diagram of the proposed system is as shown in Fig. 5.1 An optical field in the form of Gaussian pulse with 20 ns pulse width, peak power at 2 W is input into the system. The large bandwidth signals can be seen within the second micror ing device, and shown in Fig. 5.2 The suitable ring parameters are used, for instance, ring radii R_1= 16.0 μm, R_2= 5.0 μm, and R_d= 25.0 μm. In order to make the system associate with the practical device [67,68], the selected parameters of the system are fixed to λ_0 = 400 nm, n_0 = 3.34 (**InGaAsP/InP**), A_{eff} = 0.50, 0.25 μm^2 for a micro ring and add/drop ring resonator, respectively, α = 0.5 dBmm^{-1}, γ = 0.1. The coupling coefficient (kappa, κ) of the micro ring resonator ranged from 0.55 to 0.90. The nonlinear refractive index of the micro ring is n_2=2.2 x 10^{-17} m^2/W. In this case, the wave guided loss used is 0.5dBmm^{-1}. The input Gaussian pulse is chopped (sliced) into a smaller signal spreading over the spectrum as shown in Fig. 5.2 (b) and (c), which is shown that the large bandwidth signal is generated within the

second ring device. The signal amplification is occurred within the second micro ring resonator, the maximum output of 500 W is obtained as shown in Fig, 5.2(c). In applications, the specific output wavelength range can be filter after the second ring by using the add/drop filter device. We have found that the large bandwidth signal can be selected(filtered) as shown in Fig. 5.2(d), the output signal with free spectrum range(FSR) and spectral width(Full Width at Half Maximum, FWHM) of 381 nm and 30 nm are obtained, respectively. Similarly, more results of the different center wavelengths are shown in Figs. 5.3-5.6.

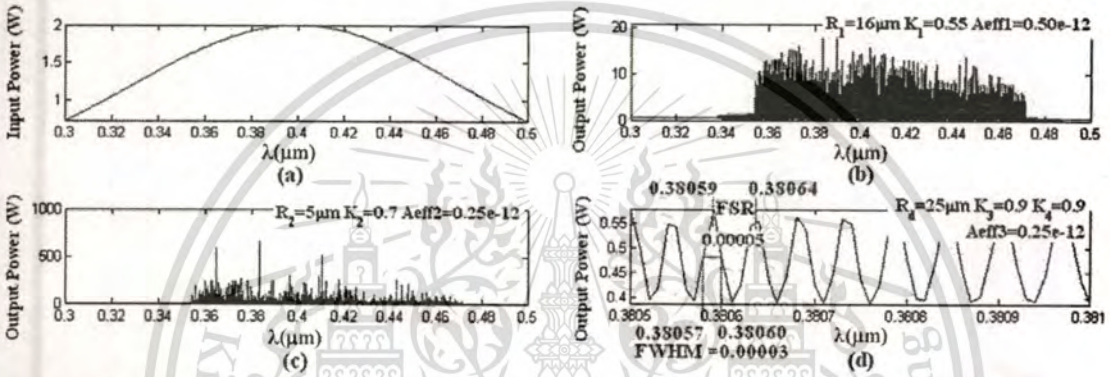

Fig. 5.2 Results of the spatial pulses with center wavelength at 400 nm, where (a) the input Gaussian pulse, (b) the large bandwidth signal, (c) the filtering and amplifying signals, (d) the drop port signals.

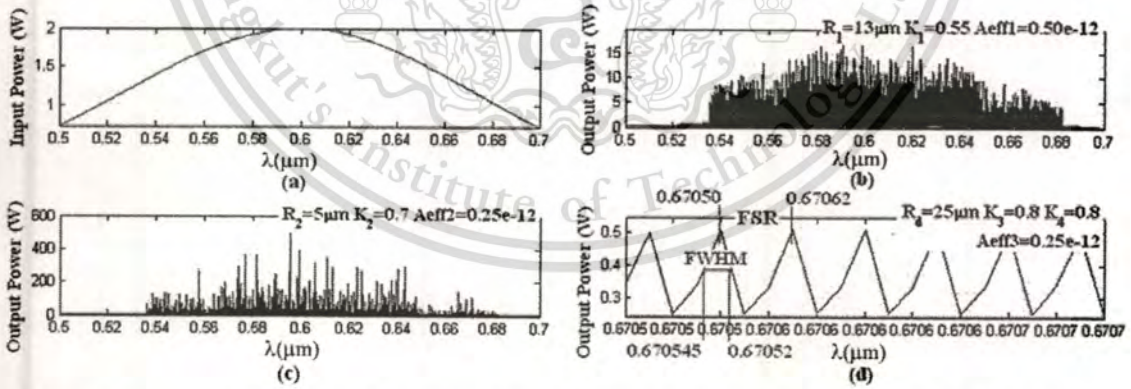

Fig. 5.3 Results of the spatial pulses with center wavelength at 600 nm, where (a) the input Gaussian pulse, (b) the large bandwidth signal, (c) the filtering and amplifying signals, (d) the drop port signals.

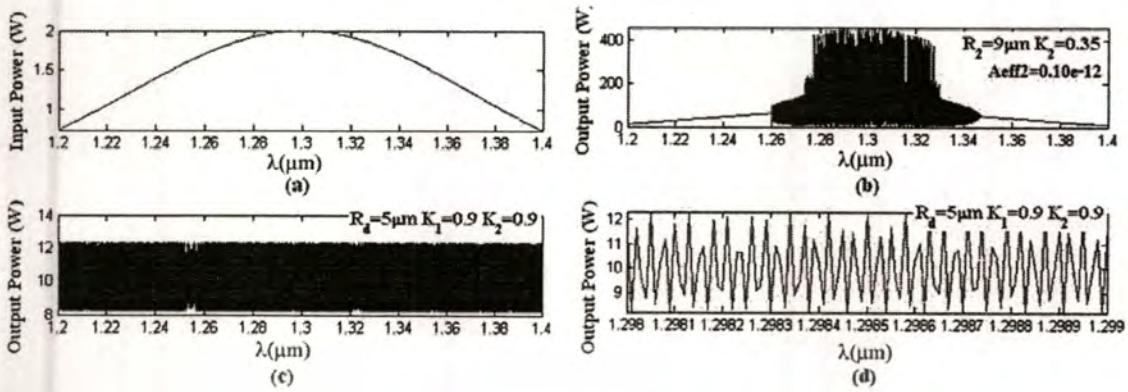

Fig. 5.4 Results of the spatial pulses with center wavelength at 1,300 nm, where (a) the input Gaussian pulse, (b) the large bandwidth signal, (c) the filtering and amplifying signals(soliton), (d) the drop port signals.

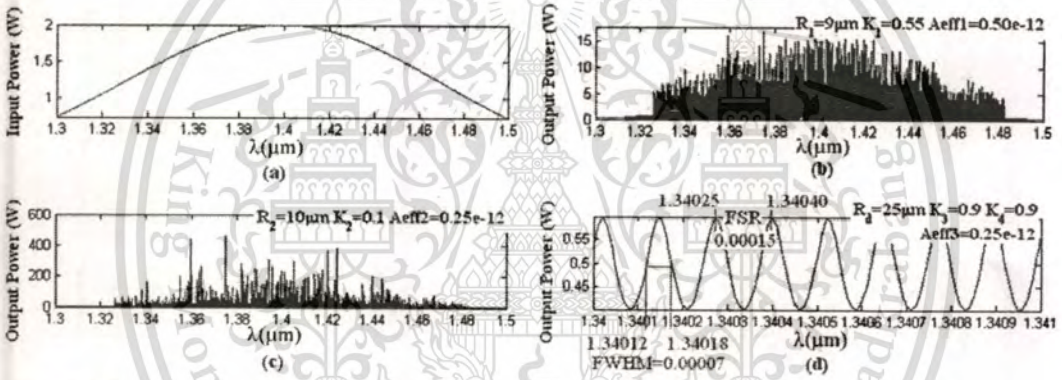

Fig. 5.5 Results of the spatial pulses with center wavelength at 1,400 nm, where (a) the input Gaussian pulse, (b) the large bandwidth signal, (c) the filtering and amplifying signals, (d) the drop port signals.

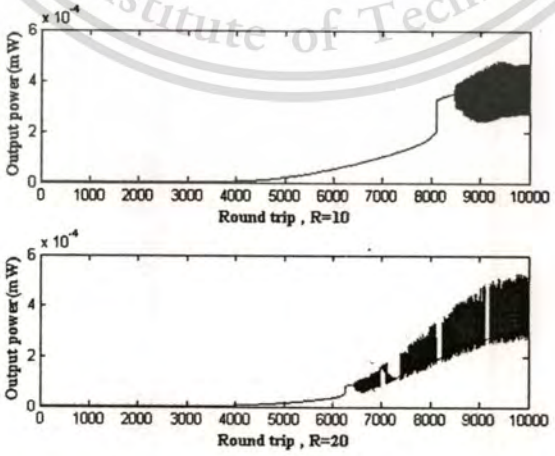

Fig. 5.6 Shows the nonlinear behaviors of light in a micro ring resonator with (a) R=10 μm and (b) R=20 μm.

This nonlinear behavior of light traveling in a single ring resonator (SRR) was investigated, where the parameters of the system were fixed to λ_0 = 1.55 μm, n_0 = 3.34, A_{eff} = 25 μm^2, α = 0.5 dB, where the practical bending loss of the waveguide fabricated by InGaAsP/InP is confirmed by reference [26], where the propagation loss as low as 1.3±.02 dB/mm at 1.55 μm [72], γ = 0.1, and R_1 = 10 μm. The coupling coefficient of the micro ring resonator coupler was fixed in this investigation to κ = 0.0225. The nonlinear refractive index was $n_2 = 2.2 \times 10^{-15}$ m^2/W [73], and the 20,000 iterations of round-trips inside the optical fiber ring plotted. We assume that $\phi_L = 0$ for simplicity.

To design the nonlinear micro ring resonator, firstly, the nonlinear behaviour of light in the ring is required to characterize. The nonlinear behavior of the micro ring resonator with the roundtrips of 10,000 is as shown in Fig. 5.6. When the ring radius is 10 μm, the nonlinear effect is not occurred as shown in Fig. 5.6(a). It is occurred when the ring radius is 20 μm as shown in Fig. 5.6(b), where the filter characteristics have also shown.

The signals are generated by using Eq. (5.3), which can be electronically formed by the digital codes as the following details. The quantitatively present logic coding can be expressed by Eq. (5.6).

$$u(v) = \begin{cases} A, & v < 3.0\,mW \\ T, & 3.0\,mW \le v < 3.5\,mW \\ C, & 3.5\,mW \le v < 4.0\,mW \\ G, & v \ge 4.0\,mW \end{cases} \tag{5.6}$$

For instance, when $u(v)$ represents the logic states, v is the signal power. The quantization and re-quantization can be processed the similar transfer characteristics. We assume that the quantizing involved is infinite, which means that the system input signal is never clipped by saturation of the quantizing. In this case, the corresponding transfer functions of the quantizing output to its input can be expressed analytically in terms of the quantizing step size as detail in reference [74].

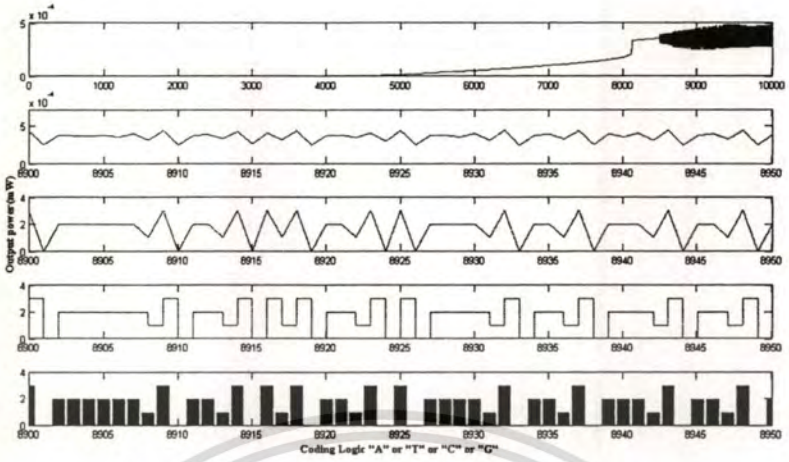

Fig. 5.7 Show the DNA codes:

[GACCCCCCTGACCTGAGTGACCTGAGACCCCTGACCTGACCCTGACCTGAC].

The DNA coding creation can be processed as the followings: (i) the signals can be generated within a ring resonator by controlling the optical input power which can be specified by the roundtrip number, i.e. time, (ii) to start the DNA coding with the threshold power, where it is marked before averaging using least-square method, (iii) the clipping signals is introduced, (iv) the DNA code generation is completed by using the approximation and sampling methods.

The first DNA codes generation is as shown in Fig. 5.7. The relationship between the output signals and roundtrips is as shown in Fig. 5.7(a), the nonlinear behavior occurs when the roundtrips number is 10,000. Fig. 5.7(b) the encoding roundtrips are from 8,900 – 8,950. Fig. 5.7(c) shows the clipping signals, 5.7(d) the clipping signals is performed by using the least- squares method, and 5.7(e) the DNA codes is obtained using the approximation method, which the logic code obtained is [GACCCCCCTGACCTGAGTGACCTGAGACCCCTGACCTGACCCTGACCT GAC], which there are 50 logic codes, a roundtrip time is 10^{-12} sec.

Similarly, Figs. 5.8 are the results which are described as the following figure captions. Fig. 5.8(a), the optical output power is 0.5 mW, with 10,000 roundtrips, where the threshold power is between 0.30 and 0.40 mW with the encoding roundtrips that range between 9050 and 9100 as shown in Fig. 5.8(b); where 5.8(c) shows the clipping signals, and the least-squares method is applied as shown in Fig. 5.8(d). There are 50 logic codes obtained with a bit time of 32 x 10^{-12} sec as shown in Fig. 5.8(e).

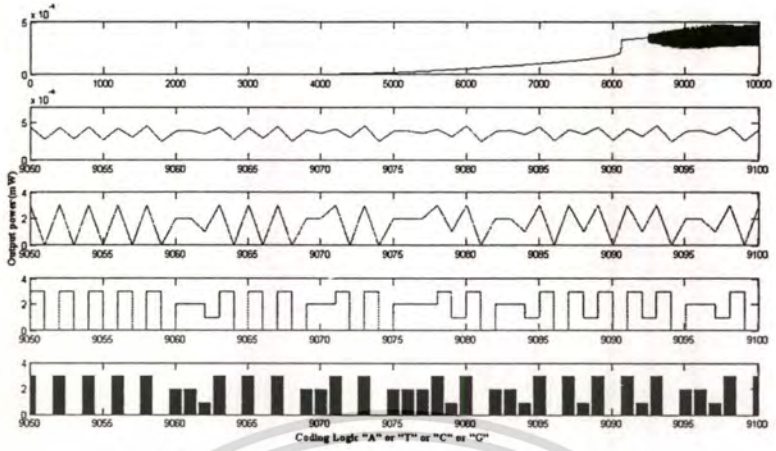

Fig. 5.8 Show the DNA codes:

[GAGAGAGAGACCTGAGAGACCGAGACCCGTGACCTGAGTGAGTGACCTGAG].

5.2 High Security Packet Switching

Consider a micro ring resonator configuration is as shown in Fig. 5.9, which is constructed by a single ring resonator and a 2x2 optical coupler [27, 75], the circumference of the micro ring is L. For convenience of analysis, we assume the complex electric field at each port as shown in Fig. 5.9 (a) is E(t), where $E_{in}(t)$ is the incoming light field of an input port and the transmitted light field to the output port is $E_{out}(t)$. While the rest of the fields $E_1(t)$ and $E_2(t)$ are the circulated fields inside the micro ring, Fig.5.9(b) shows the series micro ring resonator for design of the DNA Coding device, and Fig. 5.9(c) shows the multi-users via the micro ring resonators in optical network, where the packet switching can be performed.

This nonlinear behavior of light traveling in a single ring resonator (SRR) was investigated, where the parameters of the system were fixed to $\lambda_0 = 1.55$ μm, $n_0 = 3.34$, $A_{eff} = 25$ μm^2, $\alpha = 0.5$ dB, where the practical bending loss of the waveguide fabricated by InGaAsP/InP is confirmed by reference [26], where the propagation loss as low as 1.3±.02 dB/mm at 1.55 μm [72], $\gamma = 0.1$, and $R_1 = 10$ μm. The coupling coefficient of the micro ring resonator coupler was fixed in this investigation to $\kappa = 0.0225$. The nonlinear refractive index was $n_2 = 2.2 \times 10^{-15}$ m^2/W [73], and the 20,000 iterations of round-trips inside the optical fiber ring plotted. We assume that $\phi_L = 0$ for simplicity.

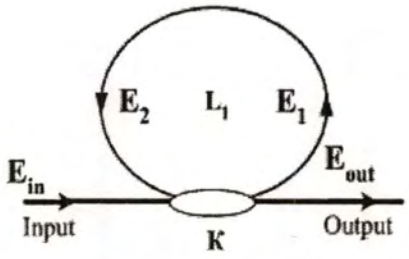

(a) a micro ring resonator.

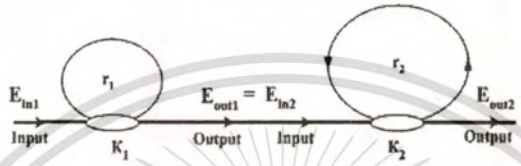

(b) the serial micro ring resonators.

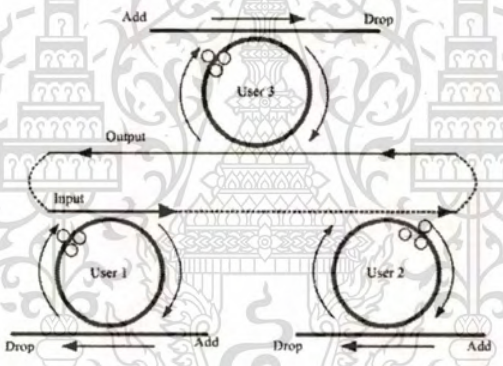

(c) the micro ring resonators in a network.

Fig. 5.9 A schematic of the micro ring resonators, (a) a micro ring resonator, (b) the serial micro ring resonators, and (c) the micro ring resonators in a network.

From Fig. 5.9(b), Eq. (5.7) is obtained by using Eq. (5.3), which is given by

$$E_{out} = (E_{in}) \sqrt{(1-\gamma)\left[1 - \frac{(1-(1-\gamma)x^2)\kappa}{(1-x\sqrt{1-\gamma}\sqrt{1-\kappa})^2 + 4x\sqrt{1-\gamma}\sqrt{1-\kappa}\sin^2(\frac{\phi}{2})}\right]} \tag{5.7}$$

When the $E_{out1} = E_{in2}$ and $K_1 = K_2$;

$$E_{out}(t) = (E_{in2}) \sqrt{(1-\gamma)\left[1 - \frac{(1-(1-\gamma)x^2)\kappa}{(1-x\sqrt{1-\gamma}\sqrt{1-\kappa})^2 + 4x\sqrt{1-\gamma}\sqrt{1-\kappa}\sin^2(\frac{\phi}{2})}\right]} \tag{5.8}$$

Using Eqs. (5.7) and (5.8), the simulation results obtained are shown in Fig. 5.10(a)-(b), and (c), respectively. The serial ring output is shown in Fig. 5.10(c), which is obtained by using a device configured in Fig. 5.9(b). However, the low level of signal to noise ratio may cause the problem in real applications.

The simulation results obtained are shown in Fig. 5.10, where Fig. 5.10(a-c) shows the generates DNA codes in the packet switching form with a ring radius of 14 μm, 15 μm, and 14 μm in series with 15 μm, respectively.

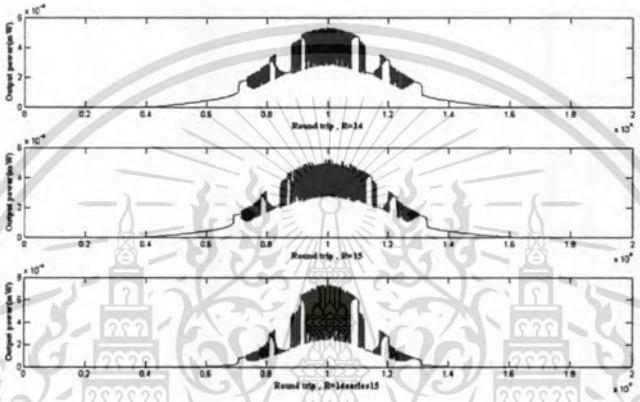

Fig . 5.10 Generates DNA codes in the Packet Switching form

The signals are generated by using Eq. (5.8), which can be electronically formed by the digital codes as the following details. The quantitatively present logic coding can be expressed by Eq. (5.6). In practice, the design micro ring resonator with its suitable parameters can be used to generate the chaotic behaviors, which are being characterized, and the DNA codes implemented.

The DNA coding creation can be processed as the followings: (i) the signals can be generated within a ring resonator by controlling the optical input power which can be specified by the roundtrip number, i.e. time, (ii) to start the DNA coding with the threshold power, where it is marked before averaging using least-square method, (iii) the clipping signals is introduced, (iv) the DNA code generation is completed by using the approximation and sampling methods.

In general, the packet switching consists of the analog to digital converter (ADC) and optical sampled and quantized ADC. The input signal is the analog signal, which is obtained from the nonlinear signal, the output signal is the digital approximation (i.e. codes) [72]. The concepts of packet switching are scheduled as follows: first step: choosing the ring resonator generation;

second step: setting the range of the DNA codes; third step: choosing to the threshold power by sampling; and final step: quantizing the analog to digital approximation.

The first DNA codes generation is as shown in Fig. 5.11. The relationship between the output signals and roundtrips is as shown in Fig. 5.11(a), the nonlinear behavior occurs when the roundtrips number is 20,000. Fig. 5.11(b) the encoding roundtrips are from 8,900 – 9,000. Fig. 5.11(c) shows the clipping signals, 5.11(d) the clipping signals is performed by using the least-squares method, and 5.11(e) the DNA codes is obtained using the approximation method, which the logic code obtained is [AAAGCAGTGTGCCACAAGAGAAATCAAATCAAGCCAAGCAGAA ATAGAGAAAGAAGCAGGAAACAAAGAAGAAGAGGAAAGCTAGGAAAGAGCTGAAAG TG] which there are 100 logic codes, a roundtrip time is 10^{-12} sec.

Similarly, Figs. 5.12 are the results which are described as the following figure captions. Fig. 5.12(a), the optical output power is 0.5 mW, with 20,000 roundtrips, where the threshold power is between 0.30 and 0.40 mW with the encoding roundtrips that range between 9000 and 9100 as shown in Fig. 5.12(b); where 5.12(c) shows the clipping signals, and the least-squares method is applied as shown in Fig. 5.12(d). There are 100 logic codes obtained with a bit time of 64 x 10^{-12} sec as shown in Fig. 5.12(e).

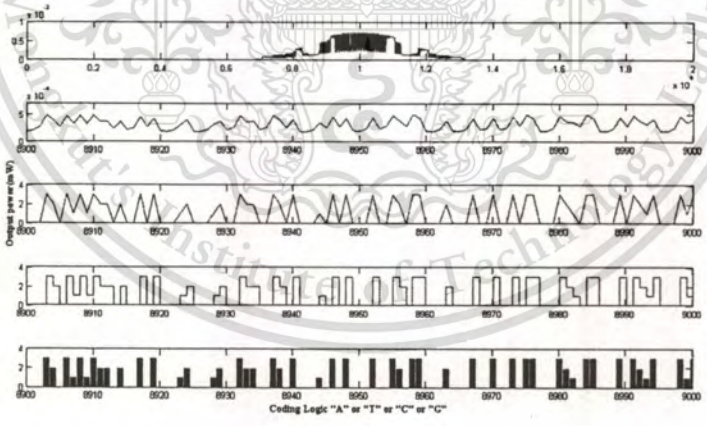

Fig. 5.11 Code DNA 8900-9000 is

AAAGCAGTGTGCCACAAGAGAAATCAAATCAAGCCAAGCAGAAATAGAGAAAGAAGC AGGAAACAAAGAAGAAGAGGAAAGCTAGGAAAGAGCTGAAAGTG

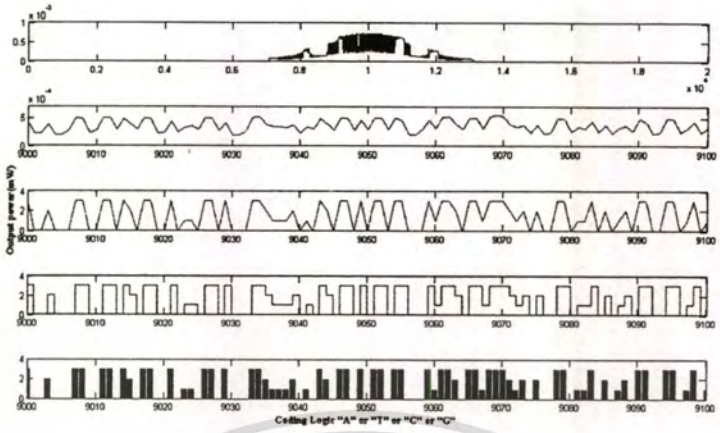

Fig. 5.12 Code DNA 9000-9100 is

GAACAAAGGAAGGAGCAGGAAGATTAGGAGAAAGGCTTTCATAGCAGGAGAGGAGGA

AAGTGGCAGGTGGGCTCACAAGGATTGACATCAGGAAGGATGAT

In operation, the generated DNA codes can be formed by quantizing the nonlinear signals, which can be switched (On/Off) to the specific users. This means the high security packet switching communication data can be performed in the optical networks. The simulation results obtained have shown that there are two schemes of the DNA codes, which can be generated to obtain the 100 logical codes.

In Fig. 5.13, the signals are generated by using the micro ring part, which the DNA codes are electronically performed by the encryption data. The signals are multiplexed and transmitted via either wire of wireless links to the required receivers. The transmitted signals are received and de-multiplexed, where the synchronously decryption to the encryption data is processed before the DNA codes being intercepted by the specific operation case.

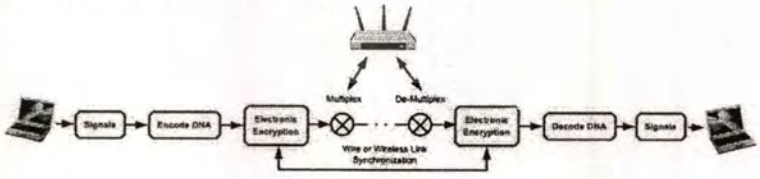

Fig. 5.13 The schematic diagram of the molecular transporter via a wavelength router in the local area network.

CHAPTER 6

CONCLUSIONS

❖ Dark – Bright Soliton Conversion

We have shown that the propagating dark soliton in the optical media can be converted to be a bright soliton by using the ring resonator system incorporating the add/drop multiplexer. By using the reasonable dark soliton input power, the output bright soliton power obtained can be used to perform the common soliton for long distance link. The advantage is that the detection of the dark soliton along the through port (transmission line) is difficult, while the detection of the bright one (by the specific user) can be performed by the standard form. This means the use of dark soliton to form the signal security or communication security is plausible, which is also available for network security application. The dark-bright signal amplification can also be used to use in long distance communication link with security applications.

❖ Storage and Tunable Light Source Generation

We have shown that a broadband light source at the specific center wavelength can be generated, stored and regenerated. The storage of broadband light source within a storage ring (R_s or R_4). The maximum stored power of 100 W, where the average optical output power of 4.0 W is achieved via an add/drop filter. The spectral width, i.e. full width at half maximum (FWHM) and free spectrum range (FSR) of 50 pm and 500 pm, which is allowed the increasing in channel capacity of 10,000 times in a single center wavelength. In application, the problem of the signal interference, i.e. collision, can be managed by using the appropriate free spectrum range design.

❖ DNA Codes Generation

We have proposed the use of a micro ring resonator to generate the DNA codes, where the advantages of such a device are (1) the signal are randomly encoded, (2) easy to design an implement, and finally (3) the control optical power could be selected. In an application, such a proposed device can be fabricated and implemented in the communication. For examples, an access point, optical wireless LAN, computing system, and computer networks. The signal can be encoded by using the electronically synchronized technique, where the required message can be successfully decoded by subtracting the oscillation. This is operated by the receiver on the

transmitted signal by using the least-squares method. We have demonstrated that the signal is logically encoded by using the waveforms of the transmitter and signal of the receiver output. Thus, we can use the proposed system for the alternative security technique that can provide the secure transmission of a message by logical coding using the electronic quantizing, and coding by using the micro ring incorporating in the communication transmission.

❖ High Security Packet Switching

The device based micro ring resonator can be used to generate the DNA codes, where the advantages are the signals randomly encoded, ease to design and implement by controlling optical power. In application, such device can be fabricated and implemented in the computer network, for examples, an access point, optical wireless LAN, computing system, and DNA computer. The signal can be encoded by using the electronically synchronized technique, where the required message can be successfully decoded by subtracting the oscillation. This is operated by the receiver on the transmitted signal by using the least-squares method. The DNA coding signal is logically encoded by using the waveforms of the transmitter and DNA encoding signal of the receiver output. Thus, we can conduct a secure transmission of a message and logical coding using the quantizing and DNA coding. However, the long distance link when the loss in optical power is the issue of implementation, then the optical repeater is required into the system, where the signal recovery and noise reduction are required to be taken into account.

In practice, such a proposed device can be fabricated and implemented in the computer networks, which can be formed the high security packet switching by using the DNA coding signals; for examples, such device can be applied into the optical wireless link, an access point, computing system, and DNA computer. For further application, the more advantage method which is called DNA computer may be the new area of investigation in the near future.

In conclusions, the future trend of using such present work is discussed, where the application such as Fuzzy Coding and super high channel capacity for optical wireless link will also be discussed as well.

LIST OF PUBLICATIONS

1. W. Siririth, S. Mitatha, O. Pingern, and P.P. Yupapin, **"A novel temporal dark-bright solitons conversion system via an add/drop filter for signal security use"**, International Journal of Light and Electron Optics, 2009. (Impact Factor:2008:0.507) (Article in press)

2. W. Siririth, S. Mitatha, and P.P. Yupapin, **"Novel storage and tunable light source generated by a soliton pulse in a micro ring resonator system"**, International Journal of Light and Electron Optics, 2009. (Impact Factor:2008:0.507) (Article in press)

REFERENCES

[1] R.W. Eason and A. Miller. **"Nonlinear optics in signal processing."** London, U.K.: Champan & Hall, 1993

[2] M. N. Islam. **"Fiber switching devices and systems."** New York, NY: Cambridge University Press, 1992

[3] E. Cotter, J. K. Lucek, and D. D. Marcenac. "Ultra-high-bit-rate networking: From the transcontinental backbone to the desktop." **IEEE Comm. Mag.**, vol. 34, 1997. pp. 90-95

[4] P. P. Mitra and J. B. Stark. "Nonlinear limits to the information capacity of optical fiber communications." **Nature**, vol. 411, 2001. pp. 1027

[5] P. W. Smith. "On the physical limits of digital optical switching and logic elements." **The Bell Sys. Tech. J.**, vol. 61, 1982. pp. 1975-1983

[6] L. Brzozowski and E. H. Sargent. "Nonlinear distributed-feedback structures as passive optical limiters." **J. Opt. Soc. of America B.**, vol. 17, 2000. pp. 1360-1365

[7] L. Brzozowski and E. H. Sargent. "Optical signal processing using nonlinear distributed feedback structures." **IEEE J. Quantum Electron.**, vol. 36, 2000. pp. 550-555

[8] L. Brzozowski and E. H. Sargent. "Nonlinear disordered media for broad-band optical limiting." **IEEE J. Quantum Electron.**, vol. 36, 2000. pp. 1237-1242

[9] P. W. Smith, I. P. Kaminov, P. J. Maloney, and L. W. Stulz. "Self-contained integrated bistable optical devices." **Appl. Phys. Lett.**, vol. 34, 1979. pp. 62-65

[10] P. W. Smith and E. H. Turner. "A bistable Farbry-Perot resonator." **Appl. Phys. Lett.**, vol. 30, 1977. pp. 280-281

[11] B. E. A. Saleh and M. C. Teich. **"Fundamentals of Photonics."** New York: Wiley, 1991

[12] P. W. E. Smith and L. Qian. "Switching to optical for a faster tomorrow." **IEEE Circuits and Devices Mag.**, vol. 15, 1999. pp. 28-33

[13] P. W. E. Smith. "All-optical devices: materials requirements." in **Nonlinear Opt. Prop. Adv. Mats.**, vol. 1852, 1993. pp. 2-9

[14] G. I. Stegeman. "All-optical devices: materials requirements." in **Nonlinear Opt. Prop. Adv. Mats.**, vol. 1852, 1993. pp. 75-89

[15] I. C. Khoo, M. Wood, and B. D. Guenther. "Nonlinear liquid crystal optical fiber array for all-optical switching/limiting." in **LEOS '96 9th Annual Meeting**, vol. 2, 1996. pp. 211-212

[16] G. L. Wood, W. W. Clark III, M. J. Miller, G. J. Salamo, and E. J. Sharp. "Evaluation of passive optical limiters and switches." in **Materials for Optical Switches, Isolators, and Limiters,** vol. 1105, 1989. pp. 154-181

[17] R. Bozio, M. Meneghetti, R. Signorini, M. Maggini, G. Scorrano, M. Prato, G. Brusatin, and M. Guglielmi. "Optical limiting of fullerene derivatives embedded in sol-gel materials." in **Photoactive Organic Materials. Science and Applications. Proceedings of the NATO Advanced Research Workshop,** vol. 572, 1996. pp. 159-174

[18] R. Wang and K. Shen, "Synchronization of chaotic systems modulated by another chaotic system in an erbium-doped fiber dual-ring laser system" **IEEE J. Quantum Electron.** Vol.37, 2001. pp. 960-967

[19] R.W. Tkach, A. R. Chraplyvy, F. Forghieri, A. H. Gnauck, and R. M. Derosier, "Four-Photon Mixing and High-Speed WDM Systems," **Journal of Light wave Technology**, Vol. 13, 1995. pp. 841–849

[20] C. Juang,T.M. Hwang, J.Juang,and Wen-wei Lin. "A Synchronization Scheme using self-pulsating laser diode in optical chaotic communication ". **IEEE J. Quantum Electron.,** Vol. 36, 2000. pp. 300-304

[21] F.Y. Lin and M.C. Tsai, " Chaotic communication in radio-over-fiber transmission based on optoelectronic feedback semiconductor lasers," **Opt. Exp.** , Vol. 15, 2007. pp. 302-309

[22] G.D. Van Wiggeren and R. Roy, "Optical Communication with Chaotic Wave forms", **Phys. Rev. Lett.** ,Vol. 81, 1998. pp. 3547-3551

[23] K. Ikeda, H. Daido and O. Akimoto, "Optical Turbulence: Chaotic Behavior of Transmitted Light from a Ring Cavity," **Phys. Rev. Lett.** ,Vol. 45, 1980. pp. 709-715

[24] F. Morichetti and A. Melloni, " Polarization converters based on ring-resonator phase-shifters," **IEEE J. Photon. Technol. Lett.**, Vol. 18, 2006. pp. 923-928

[25] M.K. Chin, C. Xu and W. Huang, " Chaotic oscillations of the optical phase for multigigahertz-bandwidth secure communications" **Opt. Exp.** Vol. 12, 2004. pp. 3245

[26] T. Aizawa, K.G. Ravikumar, Y. Nagasawa, T. Sekiguchi and T. Watanabe, "InGaAsP/InP NQW direction couple switch with small and low-loss bends for fiber array coupling," **IEEE Photonics Technol. Lett.,** Vol. 6(1994)709-711.

[27] P.P. Yupapin and W. Suwancharoen, "Chaotic signal generation and cancellation using a microring resonator incorporating an optical add/drop multiplexer," **Opt. Commun.,** 280(2)(2007)343-350.

[28] A. Morand, Y. Zhang, B. Martin, K. P. Huy, D. Amans and P. Benech, "Ultra-compact microdisk resonator filters on SOI substrate", **Opt. Exp.,** Vol. 14, No. 26(2000)12814-12821.

[29] V. Van, T.A. Ibrahim, P.P. Absil, F.G. Jhonson, R. Grover and P. T. Ho, "Optical signal processing using nonlinear semiconductor microring resonators", **IEEE J. Quantum Electron.,** 8(2002)705-713.

[30] R. W. Boyd. "**Nonlinear Optics.**" 2nd ed. Academic Press, Inc., 2003

[31] G.P. Agrawal. "**Nonlinear Fiber Optics.**" Academic Press, San Diego, CA, 2001

[32] D. A. B. Miller, S. D. Smith, and A. Johnston. "Optical bistability and signal amplification in a semiconductor crystal: Applications of new low-power nonlinear effects in InSb." **Appl. Phys Lett.,** vol. 35, no. 12, 1979. pp. 658–660

[33] P. Mandel, S. Smith, and B. Wherrett. "**From Optical Bistability Towards Optical Computing.**" North-Holland, 1987

[34] H. M. Gibbs. "**Controlling Light with Light.**" Academic Press Inc., 1985

[35] K. Otsuka. "Pitchfork bifurcation and all-optical digital signal processing with a coupled-element bistable system." **Opt. Lett.,** vol. 14, no. 1, 1989. pp. 72-74

[36] L. M. Zhao, D. Y. Tang, F. Lin and B. Zhao. "Observation of period-doubling bifurcations in a femtosecond fiber soliton laser with dispersion management cavity." **Opt. Exp.** vol. 12, no. 19, 2004. pp.4573-4578

[37] A. Hasegawa and Y. Kodama. "Signal transmission by optical solitons in monomode fiber." **Proc. IEEE.,** vol. 69, no. 9, Sept 1981. pp.1145–1150

[38] S. Blair. "**Optical soliton-based logic gates.**" Ph.D. dissertation, University of Colorado, 1998

[39] E. Infeld and G. Rowlands. "**Nonlinear waves solitons and chaos.**" Cambridge university press, 2000

[40] P.P. Yupapin, P. Phiphithirankarn and S. Suchat, "A Quantum CODEC Design via an Optical Add/Drop Multiplexer in a Fiber Optic Network," **Far East Journal of Electronics and Communications**, Vol. 1, 2007. pp. 259-267

[41] E. A. J. Marcatili. "Bends in Optical Dielectric Guides." **Bell. Syst. Tech. J.**, vol. 48, September1969. pp. 2103-2132.

[42] E. A. J. Marcatili. "Dielectric Rectangular Waveguide and Directional Coupler for Integrated Optics." **Bell. Syst. Tech. J.**, vol. 48, September 1969. pp. 2071-2101.

[43] C. K. Madsen and J. H. Zhao. "A General Planar Waveguide Autoregressive Optical Filter." **IEEE J. Lightwave Tech.**, vol. 14, no. 3, March 1996. pp. 437-447

[44] S. C. Hagness et al.. "FDTD Microcavity Simulations: Design and Experimental Realization of Waveguide-Coupled Single-Mode Ring and Whispering-Gallery-Mode Disk Resonators." **IEEE J. Lightwave Tech.**, vol. 15, no. 11, November 1997. pp. 2145-2165

[45] D. Rafizadeh et al.. "Waveguide-coupled AlGaAs/GaAs microcavity ring and disk resonators with high finesse and 21.6 nm free spectral range." **Opt. Lett.**, vol. 22, no. 16, August 1997. pp. 1244-1246

[46] B. E. Little et al.. "Ultra-Compact Si-SiO_2 Microring resonator Optical Channel Dropping Filters." **IEEE Photon. Techn. Lett.**, vol. 10, no. 4, April 1998. pp. 549-551

[47] D. J. W. Klunder et al., "Vertically and laterally waveguide-coupled cylindrical microresonators in Si_3N_4 on SiO_2 technology." **Appl. Phys. B 73.**, November 2001. pp. 603-608

[48] B. Vanderhaegen et al.. "High Q GaInAsP ring resonator filters." **ECIO'99**, Torino Italy, April 1999. pp. 381-384

[49] M. K. Chin et al.. "GaAs Microcavity Channel-Dropping Filter based on a Race-Track Resonator." **IEEE Photon. Techn. Lett.**, vol. 11, no. 12, December 1999. pp. 1620-1622

[50] C. K. Madsen and J. H. Zhao, "**Optical Filter Design and Analysis: A Signal Processing Approach.**" New York: Wiley, 1999

[51] J. E. Heebner and R.W. Boyd. "Enhanced all-optical switching by use of a nonlinear fiber ring resonator." **Opt. Lett.**, vol. 24, no. 12, 1999. pp. 847–849

[52] Mário F. S. Ferreira, "Nonlinear Effects in Optical Fibers: Limitations and Benefits," **Proc. SPIE,** 6793, 02(2007).

[53] P.P. Yupapin, W. Suwanchareon and S. Suchat, "Nonlinearity Penalties and Benefits of Light Traveling in a Fiber Optic Ring Resonator," **Int. J. of Light and Electron Opt.,** 2007. DOI : 10.1016/j.ijleo.2007.07.009.9Available online).

[54] P.P. Yupapin and N. Pornsuwancharoen, **Guided Wave Optics and Photonics: Micro Ring Resonator Design for Telephone Network Security,** Nova Science Publishers, New York, 2008.

[55] P.P. Yupapin and P. Saeung, **Photonics and Nanotechnology,** World Scientific, Singapore, 2008.

[56] Y. Su, F. Liu and Q. Li, "System Performance of Slow-light Buffering and Storage in Silicon Nano-waveguide," **Proc. SPIE,** 6783, 68732P(2007).

[57] P.P. Yupapin, N. Pornsuwanchroen and S. Chaiyasoonthorn, "Attosecond Pulse Generation using Nonlinear Micro Ring Resonators," **Microw. and Opt. Technol. Lett.,** 50, 3108(2008).

[58] Y. S. Kivshar and B. Luther-Davies, "Dark optical solitons: Physics and applications," **Phys. Rep.,** 298(1998)81-197.

[59] W. Zhao and E. Bourkoff, "Propagation properties of dark solitons," **Opt. Lett.,** 14(1989)703-705.

[60] N. Pornsuwanchroen, S. Chaiyasoonthorn and P.P. Yupapin, "Fast and slow lights generation using chaotic signals in the nonlinear micro ring resonators for communication security," **Opt. Eng.,** 49(1), 2009, in press.

[61] N. Q. Ngo, "Proposal for a high-speed optical dark-soliton detector using a microring resonator," **IEEE Photon. Technol. Lett.,** 19(2007)471-473.

[62] I.V. Barashenkov, "Stability criterion for dark soliton," **Phys. Rev. Lett.,** 77(1996) 1193-1197.

[63] D. N. Christodoulides, T. H. Coskun, M. Mitchell, Z. Chen and M. Segev, "Theory of incoherent dark solitons," **Phys. Rev. Lett.,** 80(1998)5113-5116.

[64] A. D. Kim, W. L. Kath and C. G. Goedde, "Stabilizing dark solitons by periodic phase-sensitive amplification," **Opt. Lett.**, 21(1996)465-467.

[65] B. A. Malomed, A. Mostofi and P. L. Chu, "Transformation of a dark soliton into a bright pulse," **J. Opt. Soc. Am. B**, 17(2000)507-513.

[66] N. Pornsuwancharoen and P.P. Yupapin, "Generalized fast, slow, stop and store light optically within a nano-ring resonator," **Microw. and Opt. Technol. Lett.**, 51(4), 2009, in press.

[67] C. Fietz and G. Shvets, "Nonlinear polarization conversion using micro ring resonators," **Opt. Lett.**, 32(2007) 1683-1685.

[68] Y. Kokubun, Y. Hatakeyama, M. Ogata, S. Suzuki, and N. Zaizen, "Fabrication technologies for vertically coupled micro ring resonator with multilevel crossing busline and ultracompact-ring radius," **IEEE J. of Sel. Topics in Quantum Electron.**, 11(2005)4-10.

[69] P.P. Yupapin and N. Pornsuwanchroen, "Proposed nonlinear micro ring resonator arrangement for stopping and storing light," **IEEE Photon. Technol. Lett.**, 21, 404-406(2009).

[70] D. Deng and Q. Guo, "Ince-Gaussian solitons in strongly nonlocal nonlinear media", **Opt. Lett.**, 32(2007)3206-3208.

[71] P.P. Yupapin, P. Saeung and C. Li, "Characteristics of complementary ring-resonator add/drop filters modeling by using graphical approach", **Opt. Commun.**, 272(2007)81-86.

[72] S. Xiao, M.H. Khan, H. Shen and M. Qi, "Compact silicon micro ring resonators with ultra-low propagation loss in the C band", **Opt. Exp.**, 15(22)(2007)14467- 14475.

[73] B.E. Little, S.T. Chu, J.V. Hryniewicz, and P.P. Absil, "Filter synthesis for periodically coupled micro ring resonators", **Opt. Lett.**, 25(5)(2000)344-346.

[74] G.C. Valley, "Photonic analog-to-digital converters," **Opt. Exp.**, 15(5)(2007)1955-1982.

[75] P.P. Yupapin, P. Saeung and W. Suwancharoen, "Coupler-loss and coupling-coefficient dependence of bistability and instability in a fiber ring resonator: nonlinear behaviors", **J. of Nonlinear Optical Physics & Materials(JNOPM)**, 16(2007)111-118.

APPENDIX

Full Paper's Publications

1. W. Sririth, S. Mitatha, O. Pingern, and P.P. Yupapin, **"A novel temporal dark-bright solitons conversion system via an add/drop filter for signal security use",** International Journal of Light and Electron Optics, 2009. (Impact Factor:2008:0.507) (Article in press)

2. W. Sririth, S. Mitatha, and P.P. Yupapin, **"Novel storage and tunable light source generated by a soliton pulse in a micro ring resonator system",** International Journal of Light and Electron Optics, 2009. (Impact Factor:2008:0.507) (Article in press)

Optik ▮ (▮▮▮▮) ▮▮▮–▮▮▮

Contents lists available at ScienceDirect

Optik

journal homepage: www.elsevier.de/ijleo

A novel temporal dark-bright solitons conversion system via an add/drop filter for signal security use

W. Siririth [a], S. Mitatha [a], O. Pingern [b], P.P. Yupapin [c,*]

[a] Hybrid Computing Research Laboratory, Faculty of Engineering King Mongkut's Institute of Technology Ladkrabang, Bangkok 10520, Thailand
[b] Faculty of Science, Ramkhamhaeng University, Bangkok 10400, Thailand
[c] Advanced Research Center for Photonics, Faculty of Science King Mongkut's Institute of Technology Ladkrabang, Bangkok 10520, Thailand

ARTICLE INFO

Article history:
Received 20 January 2009
Accepted 17 May 2009

Keywords:
Communication security
Dark and bright soliton
Micro-ring resonator
Optical communication

ABSTRACT

We propose a new design of a security scheme by using the nonlinear behaviors of temporal dark and bright solitons within a micro-ring resonator system for signal security application. When a dark soliton pulse is input into the proposed system, the chaotic signal is generated, where the required bright soliton pulse can be retrieved and detected by the add/drop filtering device. The chaotic wave form can be cancelled by using an add/drop device, which can be connected and used in the communication link. By using the appropriate ring parameters, simulation results obtained have shown that the soliton conversion can be performed. The ring radii used are within the ranges from 5 to 10 μms and A_{eff} = 0.10–0.50 μm². In application, the chaotic signal is generated and formed by the dark soliton within a nonlinear micro-ring device. This can be seen by using the add/drop device, where the bright soliton is formed and detected, which is available to use in communication link. The different temporal soliton response time is seen, the response times of 169 and 84 ns are noted for temporal dark and bright solitons, respectively, which can also be used to form the security key.

1. Introduction

Dark and bright soliton behaviors have been widely investigated in different forms [1,2]. The use of soliton, i.e. bright soliton in long-distance communication link has been implemented for nearly two decades, however, the interesting works using bright solitton in communication remain, whereas the use a soliton pulse within a micro-ring resonator for communication security has been studied [3]. The interesting results are when the technique could be implemented within a tiny device such as a micro-ring and nano-ring resonators and could be implemented within the mobile hand set [3,4]. Dark soliton is one of the soliton properties, whereas the soliton amplitude is vanished or minimized during the propagation in media, therefore, the dark soliton detection is difficult. The investigation of dark soliton behaviors has been reported [5,6], where one point of them has shown the interesting results, where the dark soliton can be stabilized [7] and converted into bright soliton [8] and finally detected. This means that we can use the dark soliton penalty due to the low level of the peak power to be the benefit, where the promising idea is that a dark soliton can be performed the communication transmission carrier where the recovery can be retrieved by the dark-bright soliton conversion. Actually, we are looking for the simple technique that can be employed to detect the dark soliton. Yupapin and Suwancharoen [9] have reported the interesting results of light pulse propagating within a nonlinear micro-ring device, where the transfer function of the output at the resonant condition is derived and used. They found that the broad spectrum of light pulse can be transformed to the discrete pulses. Recently, Pornsuwancharoen and Yupapin [10] have reported that a soliton pulse can be localized within a nano-waveguide, where they have design a system, which is consisted of micro- and nano-ring resonators, the soliton pulse can be stored within the nano-waveguide. In this paper, we have shown that after the clean dark soliton is input and chopped to be the noisy signals for security purpose within the nonlinear ring resonator system, which can be transmitted into the transmission link safely. The required users can retrieve the original signal via an add/drop filter, where they can chose to retrieve in either bright or dark soliton pulses. However, the device parameters are the given keys for the end users, where they can use to form the device that can be used to retrieve the signals in the link or network.

An optical soliton is recognized as a powerful laser pulse, which can be used to enlarge the optical bandwidth when propagating within the nonlinear micro-ring resonator [10]. Moreover, the superposition of self-phase modulation soliton pulses can keep the large output power. Initially, the optimum energy is coupled into the waveguide by a lager effective core area device, i.e. micro-ring resonator. Then the smaller one is connected to transfer the soliton power, however, the optical loss

* Corresponding author.
E-mail address: kypreech@kmitl.ac.th (P.P. Yupapin).

0030-4026/$ - see front matter © 2009 Elsevier GmbH. All rights reserved.
doi:10.1016/j.ijleo.2009.05.020

Please cite this article as: W. Siririth, et al., A novel temporal dark-bright solitons conversion system via an add/drop filter for signal security use, Opt. Int. J. Light Electron. Opt. (2009), doi:10.1016/j.ijleo.2009.05.020

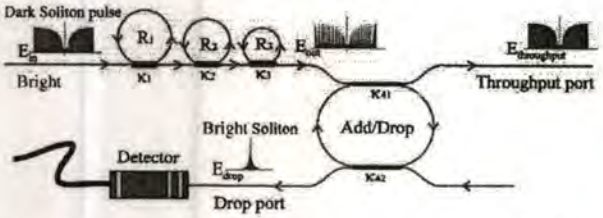

Fig. 1. A schematic of a dark-bright soliton conversion system, where R_s: ring radii, κ_s: coupling coefficients, κ_{41} and κ_{42} are the add/drop coupling coefficients.

is involved in the transferring link. The filtering characteristic of the optical signal is presented within an add/drop filter, where the suitable parameters can be controlled to obtain the required output energy. To obtain the required soliton power after propagating within the ring resonator, the suitable coupling power into the device is required, i.e. coupling coefficient (κ), whereas the interference signal is a minor effect compared to the loss associated to the direct passing through.

We are looking for a stationary dark soliton pulse, which is introduced into the multi-stage micro-ring resonators as shown in Fig. 1, the input optical field (E_{in}) of the dark soliton pulse input is given by

$$E_{in} = A\tanh\left[\frac{T}{T_0}\right]\exp\left[\left(\frac{z}{2L_D}\right) - i\omega_0 t\right] \quad (1)$$

where A and z are the optical field amplitude and propagation distance, respectively. T is a soliton pulse propagation time in a frame moving at the group velocity, $T = t - \beta_1 \times z$, where β_1 and β_2 are the coefficients of the linear and second-order terms of Taylor expansion of the propagation constant. $L_D = T_0^2/|\beta_2|$ is the dispersion length of the soliton pulse. T_0 in equation is a soliton pulse propagation time at initial input. Where t is the soliton phase shift time, and the frequency shift of the soliton is ω_0. This solution describes a pulse that keeps its temporal width invariance as it propagates, and thus is called a temporal soliton. When a soliton peak intensity ($|\beta_2/\Gamma T_0^2|$) is given, then T_0 is known. For the soliton pulse in the micro-ring device, a balance should be achieved between the dispersion length (L_D) and the nonlinear length ($L_{NL} = (1/\Gamma\phi_{NL})$, where $\Gamma = n_2 \times k_0$, is the length scale over which dispersive or nonlinear effects makes the beam becomes wider or narrower. For a soliton pulse, there is a balance between dispersion and nonlinear lengths, hence $L_D = L_{NL}$.

When light propagates within the nonlinear material (medium), the refractive index (n) of light within the medium is given by

$$n = n_0 + n_2 I = n_0 + \left(\frac{n_2}{A_{eff}}\right)P \quad (2)$$

where n_0 and n_2 are the linear and nonlinear refractive indexes, respectively. I and P are the optical intensity and optical power, respectively. The effective mode core area of the device is given by A_{eff}. For the micro- and nano-ring resonators, the effective mode core areas range from 0.50 to 0.10 μm^2 [11].

When a soliton pulse is input and propagated within a micro-ring resonator as shown in Fig. 1, which consists of a series of micro-ring resonators. The resonant output is formed, thus, the normalized output of the light field is the ratio between the output and input fields ($E_{out}(t)$ and $E_{in}(t)$) in each roundtrip, which is given by

$$\left|\frac{E_{out}(t)}{E_{in}(t)}\right|^2 = (1-\gamma)\left[1 - \frac{(1-(1-\gamma)x^2)\kappa}{(1-x\sqrt{1-\gamma}\sqrt{1-\kappa})^2 + 4x\sqrt{1-\gamma}\sqrt{1-\kappa}\sin^2(\phi/2)}\right] \quad (3)$$

The close form of Eq. (3) indicates that a ring resonator in the particular case is very similar to a Fabry–Perot cavity, which has an input and output mirror with a field reflectivity, $(1-\kappa)$, and a fully reflecting mirror. κ is the coupling coefficient, and $x = \exp(-\alpha L/2)$ represents a roundtrip loss coefficient, $\phi_0 = kLn_0$ and $\phi_{NL} = kLn_2|E_{in}|^2$ are the linear and nonlinear phase shifts, $k = 2\pi/\lambda$ is the wave propagation number in a vacuum. Where L and α are a waveguide length and linear absorption coefficient, respectively. In this work, the iterative method is introduced to obtain the results as shown in Eq. (3), similarly, when the output field is connected and input into the other ring resonators.

After the signals are multiplexed with the generated chaotic noise, then the chaotic cancellation is required by the individual user. To retrieve the signals from the chaotic noise, we propose to use the add/drop device with the appropriate parameters. This is given in details as followings. The optical circuits of ring resonator add/drop filters for the throughput and drop port can be given by [9]

$$\left|\frac{E_t}{E_{in}}\right|^2 = \frac{(1-\kappa_1) - 2\sqrt{1-\kappa_1}\sqrt{1-\kappa_2}e^{-(\alpha/2)L}\cos(k_nL) + (1-\kappa_2)e^{-\alpha L}}{1+(1-\kappa_1)(1-\kappa_2)e^{-\alpha L} - 2\sqrt{1-\kappa_1}\sqrt{1-\kappa_2}e^{-(\alpha/2)L}\cos(k_nL)} \quad (4)$$

and

$$\left|\frac{E_d}{E_{in}}\right|^2 = \frac{\kappa_1\kappa_2 e^{-(\alpha/2)L}}{1+(1-\kappa_1)(1-\kappa_2)e^{-\alpha L} - 2\sqrt{1-\kappa_1}\sqrt{1-\kappa_2}e^{-(\alpha/2)L}\cos(k_nL)} \quad (5)$$

where E_t and E_d represents the optical fields of the throughput and drop ports, respectively. $\beta = kn_{eff}$ is the propagation constant, n_{eff} is the effective refractive index of the waveguide and the circumference of the ring is $L = 2\pi R$, here R is the radius of the ring. In the following, new parameters will be used for simplification: $\phi = \beta L$ is the phase constant. The chaotic noise cancellation can be managed by using the specific parameters of the add/drop device, which the required signals can be retrieved by the specific users. κ_1 and κ_2 are coupling coefficient of add/drop filters, $k_n = 2\pi/\lambda$ is the wave propagation number for in a vacuum, and where the waveguide (ring resonator) loss is $\alpha = 0.5\,\mathrm{dB\,mm^{-1}}$. The fractional coupler intensity loss is $\gamma = 0.1$. In the case of add/drop device, the nonlinear refractive index is neglected.

In operation, a dark soliton pulse with 50 ns pulse width, the maximum power of 1.0 W is input into the dark-bright solitons conversion system as shown in Fig. 1. The suitable ring parameters are used, for instance, ring radii $R_1 = 10.0\,\mu m$, $R_2 = 7.0\,\mu m$ and $R_3 = 5.0\,\mu m$. In order to make the system associate with the practical device [12,13], the selected parameters of the system are fixed to $\lambda_0 = 1.55\,\mu m$, $n_0 = 3.34$ (InGaAsP/InP), $A_{eff} = 0.50$, 0.25 and $0.10\,\mu m^2$ for a micro- and nano-ring resonators [11], respectively, $\alpha = 0.5\,\mathrm{dB\,mm^{-1}}$, $\gamma = 0.1$. The coupling coefficients (kappa, κ) of the micro-ring resonator are ranged from 0.05 to 0.90. The nonlinear refractive index is $n_2 = 2.2 \times 10^{-17}\,m^2/W$. In this case, the wave-guided loss used is $0.5\,\mathrm{dB\,mm^{-1}}$. The input dark soliton pulse is chopped (sliced) into the smaller signals as shown in Fig. 2(a). Fig. 2(b) and (c) are the output signals of the filtering signals within the rings R_2 and R_3. We find that the output signals from R_3 are smaller than from R_1, which is more difficult to detect when it is used in the link. In fact, the multi-stage ring system is proposed due to the different core-effective areas of the rings in the system, where the effective areas can be transferred form 0.50 to $0.10\,\mu m^2$ with some losses. The soliton signals in R_3 is entered in the add/drop filter, where the dark-bright solitons conversion can be performed by using Eqs. (4) and (5). Results obtained when a dark soliton pulse is input into a micro- and nano-ring resonator systems as shown in Figs. 3 and 4. The

Please cite this article as: W. Siririth, et al., A novel temporal dark-bright solitons conversion system via an add/drop filter for signal security use, Opt. Int. J. Light Electron. Opt. (2009), doi:10.1016/j.ijleo.2009.05.020

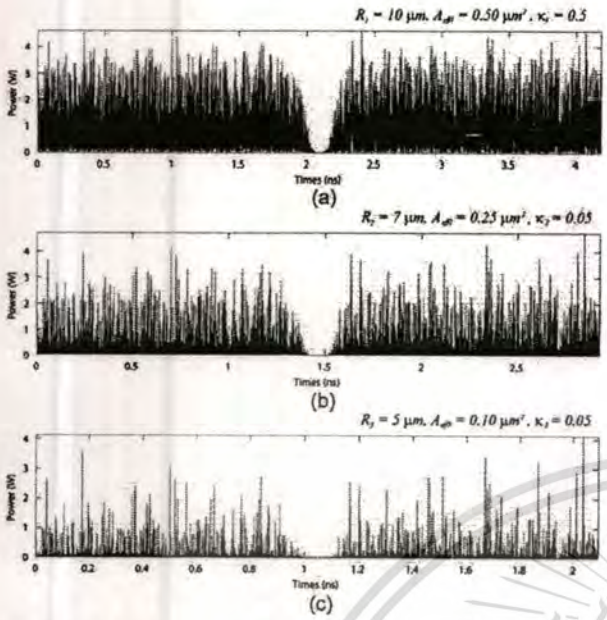

Fig. 2. Results of the soliton signals within the ring resonator system, where (a) in ring R_1, (b) in ring R_2 and (c) in ring R_3.

parameters used are the same as in Fig. 2, where the only change is the add/drop filter parameters. It is formed by two couplers and a ring radius (R_d) of 10 μm, the coupling constants (κ_{11} and κ_{12}) are the same values (0.50). When the add/drop filter is connected to the third ring (R_3), the dark-bright solitons conversion are seen. The bright soliton and dark solitons are detected by the through (throughput) and drop ports as shown in Fig. 1, respectively.

Temporal and spatial solitons are the soliton characteristics, which they present the soliton waveforms between the soliton power with time and wavelength, respectively. In the signal security concept, it is proposed by using the temporal dark soliton pulse input into the micro-ring resonator system, whereas the required signals can be multiplexed into the dark soliton pulse. The multiplexed signals, i.e. soliton pulse and the required signals are then chopped to be the noisy signals and transmitted into the link safely. Furthermore, the output soliton power, i.e. link power budget can be specified by the input dark soliton as shown in Figs. 3 and 4, the smaller input soliton power is applied, the smaller power budget is obtained. The required users can retrieve the original signal via the add/drop filter, where they can chose to retrieve in either bright or dark soliton pulses. However, the device parameters are the given keys for the end users, especially, the add/drop filter, where they can form the device that can be used to retrieve the signals in the link or network. The different temporal soliton response time is seen in Figs. 3 and 4, 5, which can also be used to form the security key where the response time of 84.65 ns is noted in this work, which is designed by the add/drop filter parameters. The response time is changed when the different add/drop filters are applied. Moreover, the power budget is also important for soliton communication concept, for instance, the output power of 500 mW is obtained as shown in Fig. 3, which is enough to operate in the link. Where more/less output power can be desired and obtained by using the appropriate initial input soliton power and the coupling coefficient (κ_1) values as in the earlier discussion. In practice, the result obtained in Fig. 4 is the best signals for security purpose among the results because the signals in ring R_3 is difficult to retrieve the original signals. The other key parameter is the radius of ring R_3, whereas the nano-waveguide is required to perform the amplified signals, i.e. soliton

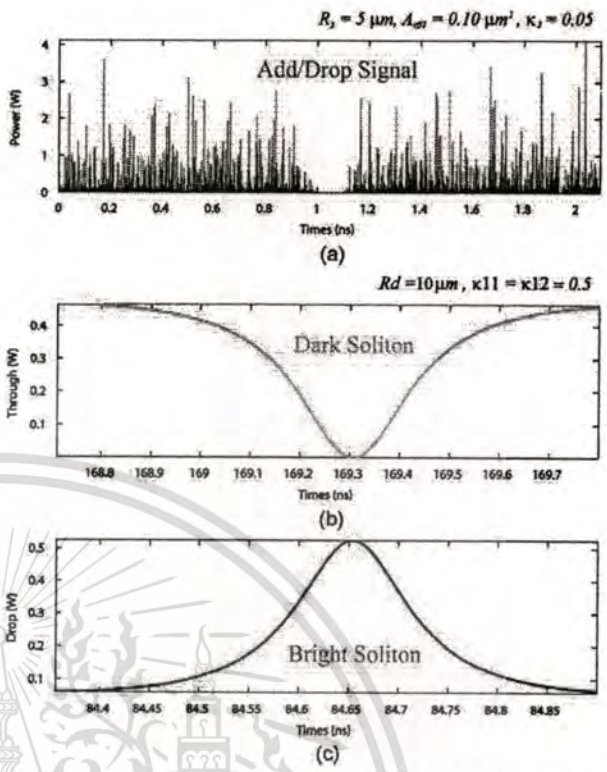

Fig. 3. Results of the optical solitons, where (a) the signals in R_3, (b) a dark soliton and (c) a bright soliton, the input dark soliton power is 1 W, $\kappa_1 = 0.5$, $R_d = 10$ mm.

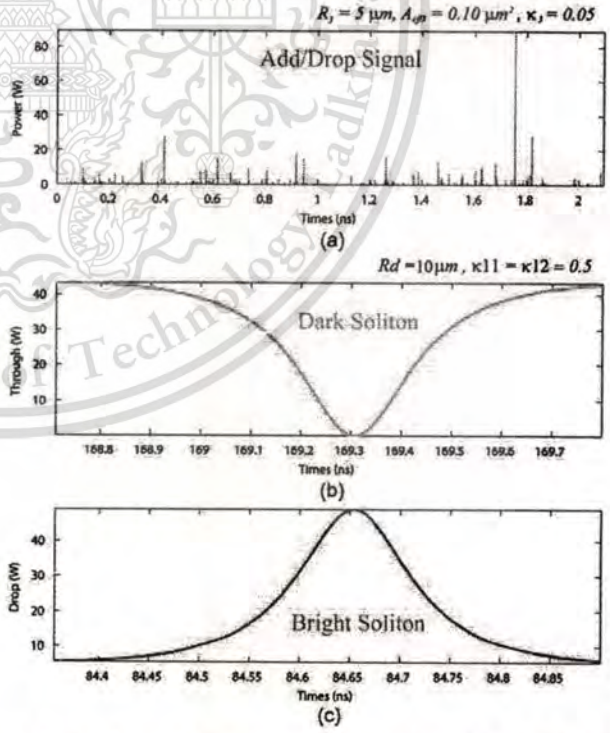

Fig. 4. Results of the optical solitons, where (a) the signals in R_3, (b) a dark soliton and (c) a bright soliton. The input dark soliton power is 1 W, $\kappa_1 = 0.9$, $R_d = 10$ mm.

pulse, for instance, the ring radius of 5 μm, with the effective core area A_{eff} of 0.10 μm² is used to obtain the nano-scale ring resonator [11].

Please cite this article as: W. Siririth, et al., A novel temporal dark-bright solitons conversion system via an add/drop filter for signal security use, Opt. Int. J. Light Electron. Opt. (2009), doi:10.1016/j.ijleo.2009.05.020

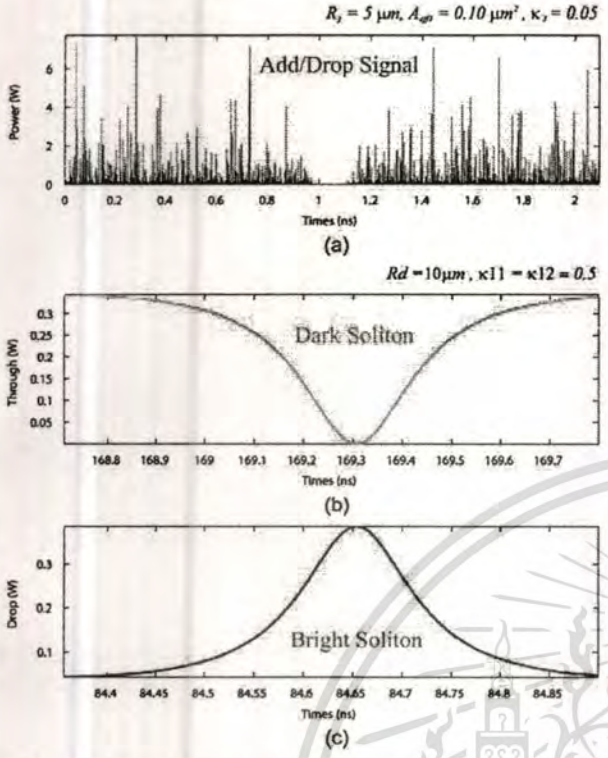

Fig. 5. Results of the optical solitons, where (a) the signals in R_3, (b) a dark soliton and (c) a bright soliton. The input dark soliton power is 1 W, $\kappa_1 = 0.4$, $R_d = 10$ mm.

In conclusion, we have shown that the propagating dark soliton in the optical media can be converted to be a bright soliton by using the ring resonator system incorporating the add/drop multiplexer. By using the reasonable dark soliton input power, the output bright soliton power obtained can be used to perform the common soliton for long-distance link, for instance, the output power of bright solitons of 0.5 and 40 W are obtained as shown in Figs. 3 and 4. The advantage is that the detection of the dark soliton along the through port (transmission line) is difficult, while the detection of the bright one (by the specific user) can be performed by the standard form. This means the use of dark soliton to form the signal security or communication security is plausible, which is also available for network security application.

Acknowledgements

One of the authors (S. Chaiyasoonthorn) would like to acknowledge the Department of Physics, Faculty of Science, Ramkhamhaeng University, Thailand for the support of his higher education at King Mongkut's Institute of Technology Ladkrabang, Bangkok, Thailand.

References

[1] Y.S. Kivshar, B. Luther-Davies, Dark optical solitons: physics and applications, Phys. Rep. 298 (1998) 81–197.
[2] W. Zhao, E. Bourkoff, Propagation properties of dark solitons, Opt. Lett. 14 (1989) 703–705.
[3] N. Pornsuwanchroen, S. Chaiyasoonthorn, P.P. Yupapin, Fast and slow lights generation using chaotic signals in the nonlinear micro ring resonators for communication security, Opt. Eng., 49(1) (2009) 015002.
[4] N.Q. Ngo, Proposal for a high-speed optical dark-soliton detector using a microring resonator, IEEE Photon Technol. Lett. 19 (2007) 471–473.
[5] I.V. Barashenkov, Stability criterion for dark soliton, Phys. Rev. Lett. 77 (1996) 1193–1197.
[6] D.N. Christodoulides, T.H. Coskun, M. Mitchell, Z. Chen, M. Segev, Theory of incoherent dark solitons, Phys. Rev. Lett. 80 (1998) 5113–5116.
[7] A.D. Kim, W.L. Kath, C.G. Goedde, Stabilizing dark solitons by periodic phase-sensitive amplification, Opt. Lett. 21 (1996) 465–467.
[8] B.A. Malomed, A. Mostofi, P.L. Chu, Transformation of a dark soliton into a bright pulse, J. Opt. Soc. Am. B 17 (2000) 507–513.
[9] P.P. Yupapin, W. Suwancharoen, Chaotic signal generation and cancellation using a micro ring resonator incorporating an optical add/drop multiplexer, Opt. Commun. 280 (2007) 343–348.
[10] N. Pornsuwancharoen, P.P. Yupapin, Generalized fast, slow, stop and store light optically within a nano-ring resonator, Microw. Opt. Technol. Lett. 51(4) (2009) 899–902.
[11] Y. Su, F. Liu, Q. Li, System performance of show-light buffering and storage in silicon nano-waveguide, Proc. SPIE 6783 (2007) 67832P.
[12] C. Fietz, G. Shvets, Nonlinear polarization conversion using micro ring resonators, Opt. Lett. 32 (2007) 1683–1685.
[13] Y. Kokubun, Y. Hatakeyama, M. Ogata, S. Suzuki, N. Zaizen, Fabrication technologies for vertically coupled micro ring resonator with multilevel crossing busline and ultracompact-ring radius, IEEE J. Sel. Top. Quantum Electron. 11 (2005) 4–10.

Please cite this article as: W. Siririth, et al., A novel temporal dark-bright solitons conversion system via an add/drop filter for signal security use, Opt. Int. J. Light Electron. Opt. (2009), doi:10.1016/j.ijleo.2009.05.020

Optik ▪ (▪▪▪▪) ▪▪▪–▪▪▪

Contents lists available at ScienceDirect

Optik

journal homepage: www.elsevier.de/ijleo

Novel storage and tunable light source generated by a soliton pulse in a micro ring resonator system

W. Siririth [a], S. Mitatha [a], P.P. Yupapin [b,*]

[a] Hybrid Computing Research Laboratory, Faculty of Engineering, King Mongkut's Institute of Technology Ladkrabang, Bangkok 10520, Thailand
[b] Advanced Research Center for Photonics, Faculty of Science, King Mongkut's Institute of Technology Ladkrabang, Bangkok 10520, Thailand

ARTICLE INFO

Article history:
Received 28 March 2009
Accepted 6 September 2009

Keywords:
Storage light source
Tunable light source
Dense light source
Dense soliton pulse

ABSTRACT

We propose a novel system of a dense wavelength division operation using the nonlinear micro ring resonators system that can be used to generate the broad output light spectra, whereas the significant increasing in channel capacity is obtained. A system consists of two micro and a nano ring resonators incorporating an add/drop filter that can be integrated into a single system. The large bandwidth signal is generated by using a soliton pulse propagating within a Kerr type nonlinear medium. The obtained results have shown the potential of using such a system for broadband light source generation, amplification, storage and regeneration, whereas the amplified signals can be stored within a nano-waveguide, which is allowed to form the regeneration of the broad light spectra after amplification. The advantage is that the specific wavelength of the broadband source, for instance, 1.50 μm can provide the super dense wavelength division multiplexing channels, whereas the increasing in channel capacity of 10,000 times is achieved.

Nonlinear device is one of the target device that should be encouraged to research for the new era of device technology. The interesting results of the use of nonlinear device have been reported recently [1,2], they have shown the interesting and promising results of using the nonlinear device known as a "nano-ring resonator" in various applications. Furthermore, the evidence of such a device using in the laboratory has also been reported [3]. Such a device is fabricated by using the nonlinear material called **"InGaAsP/InP"**, where the nonlinear refractive index value is one of the properties to obtain the good results. To begin this concept, we introduce the device known as a "ring resonator", which is in the circular form or planar waveguide, where Yupapin and Pornsuwancharoen [4] have shown that the promising application is occurred when the ring radius is down to a micrometer or nanometer scale. For instance, the ultra fast switching can be easily generated by using a remarkably simple arrangement, where the generation of the switching time of attosecond and beyond is confirmed [1]. The most interesting results are seen when light pulse can be slow down, stopped and stored within the nonlinear nano-waveguide [4], where the signal amplification within the tiny device has shown the great success. In this work, we propose two different results that can be used to form the broadband light source and store within the tiny device. Initially, a soliton pulse with center wavelength at 1.55 μm is input into the novel system, whereas the selected pulse can be filtered, amplified and stored within the nano-waveguide. Firstly, the dense wavelength source can be formed by using the stored wavelength at 1.50 μm, and secondly, it can be regenerated by using the stored wavelength at 0.50 μm. The operation system can be used to analyze and describe the concept of broadband light source generation and regeneration, which is allowed to perform the tunable light source, whereas the light source with the specific wavelength can be selected, i.e. filtered and stored.

Initially, the optimum energy is coupled into the waveguide by a lager effective core area device, i.e. ring resonator as shown in Fig. 1. Then the smaller ones are connected to form the storage unit. The filtering characteristic of the optical signal is presented within a ring resonator and an add/drop filter, where the suitable parameters can be controlled to obtain the required output spectra. To maintain the soliton pulse propagating within the ring resonator, the suitable coupling power into the device is required, whereas the interference signal is a minor effect compared to the loss associated to the direct passing through. A soliton pulse, which is introduced into the multi-stage micro ring resonators as shown in Fig. 1, the input optical field (E_{in}) of the bright soliton input is given by Eq. (1).

$$E_{in}(t)=A\,\mathrm{sech}\left[\frac{T}{T_0}\right]\exp\left[\left(\frac{z}{2L_D}\right)-i\omega_0 t\right] \quad (1)$$

where A and z are the optical field amplitude and propagation distance, respectively. T is a soliton pulse propagation time in a frame moving at the group velocity, $T=t-\beta_1^* z$, where β_1 and β_2 are

* Corresponding author.
E-mail address: kypreech@kmitl.ac.th (P.P. Yupapin).

0030-4026/$ - see front matter © 2009 Elsevier GmbH. All rights reserved.
doi:10.1016/j.ijleo.2009.11.005

the coefficients of the linear and second order terms of Taylor expansion of the propagation constant. $L_D = T_0^2/|\beta_2|$ is the dispersion length of the soliton pulse. T_0 in equation is a soliton pulse propagation time at initial input. Where t is the soliton phase shift time, and the frequency shift of the soliton is ω_0. This solution describes a pulse that keeps its temporal width invariance as it propagates, and thus is called a temporal soliton. When a soliton peak intensity ($|\beta_2/\Gamma T_0^2|$) is given, then T_0 is known. For the soliton pulse in the micro ring device, a balance should be achieved between the dispersion length (L_D) and the nonlinear length ($L_{NL}=(1/\Gamma\varphi_{NL})$), where $\Gamma = n_2^* k_0$, is the length scale over which dispersive or nonlinear effects makes the beam become wider or narrower. For a soliton pulse, there is a balance between dispersion and nonlinear lengths, hence $L_D = L_{NL}$.

When light propagates within the nonlinear material (medium), the refractive index (n) of light within the medium is given by

$$n = n_0 + n_2 I = n_0 + \left(\frac{n_2}{A_{eff}}\right)P, \tag{2}$$

where n_0 and n_2 are the linear and nonlinear refractive indexes, respectively. I and P are the optical intensity and optical power, respectively. The effective mode core area of the device is given by A_{eff}. For the micro and nano ring resonators, the effective mode core areas range 0.50–0.1 μm^2[3], where they found that fast light pulse can be slowed down experimentally after input into the nano ring.

When a soliton pulse is input and propagated within a micro ring resonator as shown in Fig. 1, which consists of a series micro ring resonators. The resonant output is formed, thus, the normalized output of the light field is the ratio between the output and input fields ($E_{out}(t)$ and $E_{in}(t)$) in each roundtrip, which can be expressed as [5]

$$\left|\frac{E_{out}(t)}{E_{in}(t)}\right|^2 = (1-\gamma)\left[1 - \frac{(1-(1-\gamma)\kappa^2)\kappa}{(1-\kappa\sqrt{1-\gamma}\sqrt{1-\kappa})^2 + 4\kappa\sqrt{1-\gamma}\sqrt{1-\kappa}\sin^2\left(\frac{\varphi}{2}\right)}\right] \tag{3}$$

The close form of Eq. (3) indicates that a ring resonator in the particular case is very similar to a Fabry–Perot cavity, which has

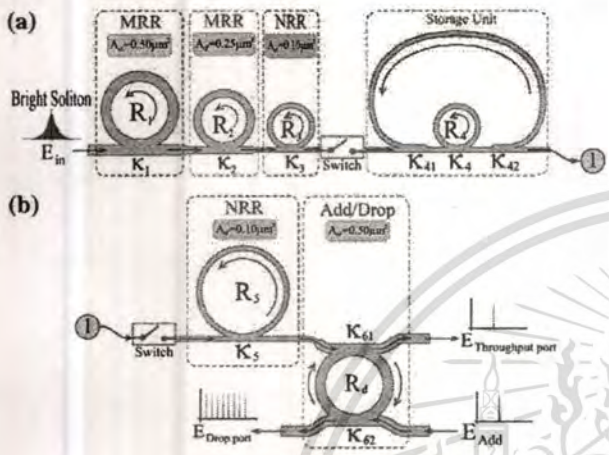

Fig. 1.]A storage and tunable light source generation system, where R_s: ring radii, κ_s: coupling coefficients, κ_{41} and κ_{42}: coupling losses κ_{61} and κ_{61} are the add/drop coupling coefficients.

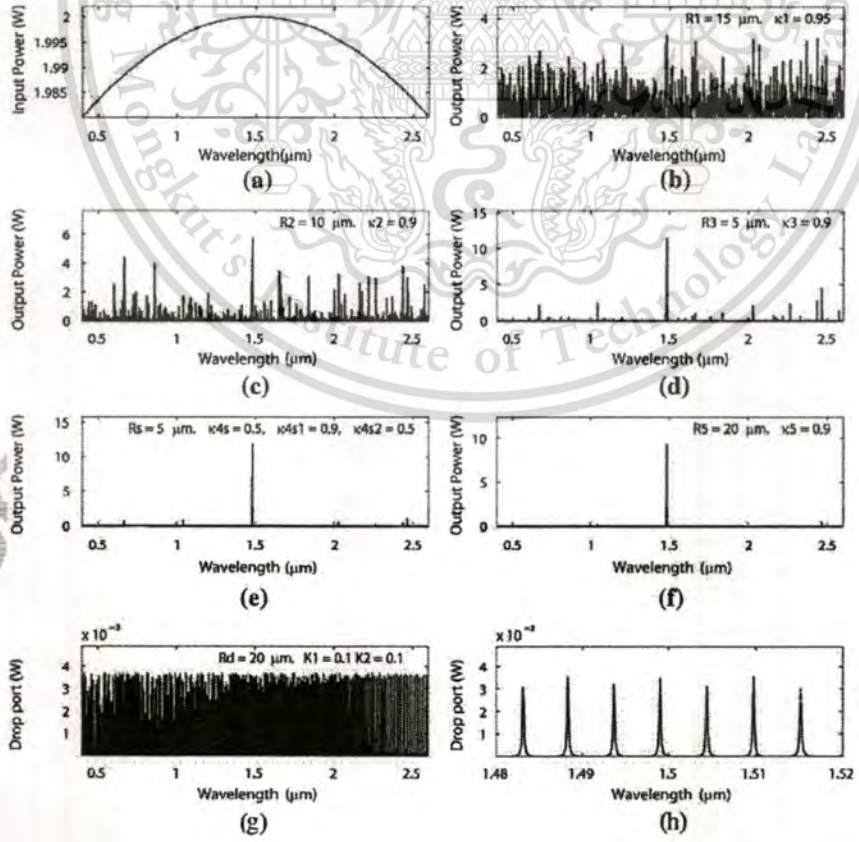

Fig. 2. Results obtained with the storage wavelength at 0.50 μm, where (a) input soliton, (b) ring R_1, (c) ring R_2, (d) ring R_3, (e) storage ring (R_s), (f) ring R_5, (g) and (h) drop port signals.

Please cite this article as: W. Sririth, et al., Novel storage and tunable light source generated by a soliton pulse in a micro ring resonator system, Opt. Int. J. Light Electron. Opt. (2009), doi:10.1016/j.ijleo.2009.11.005

an input and output mirror with a field reflectivity, $(1-\kappa)$, and a fully reflecting mirror. κ is the coupling coefficient, and $x=\exp(-\alpha L/2)$ represents a roundtrip loss coefficient, $\varphi_0=kLn_0$ and $\varphi_{NL}=kLn_2|E_{in}|^2$ are the linear and nonlinear phase shifts, $k=2\pi/\lambda$ is the wave propagation number in a vacuum. Where L and α are a waveguide length and linear absorption coefficient, respectively. In this work, the iterative method is introduced to obtain the results as shown in Eq. (3), similarly, when the output field is connected and input into the other ring resonators.

After the signals are multiplexed with the generated chaotic noise, then the chaotic cancellation is required by the individual user. To retrieve the signals from the chaotic noise, we propose to use the add/drop device with the appropriate parameters. This is given in details as followings. The optical circuits of ring-resonator add/drop filters for the throughput and drop port can be given by Eqs. (4) and (5), respectively [6].

$$\left|\frac{E_t}{E_{in}}\right|^2=\frac{(1-\kappa_1)-2\sqrt{1-\kappa_1}\sqrt{1-\kappa_2}e^{-\frac{\alpha L}{2}}\cos(k_nL)+(1-\kappa_2)e^{-\alpha L}}{1+(1-\kappa_1)(1-\kappa_2)e^{-\alpha L}-2\sqrt{1-\kappa_1}\sqrt{1-\kappa_2}e^{-\frac{\alpha L}{2}}\cos(k_nL)} \quad (4)$$

$$\left|\frac{E_d}{E_{in}}\right|^2=\frac{\kappa_1\kappa_2e^{-\frac{\alpha L}{2}}}{1+(1-\kappa_1)(1-\kappa_2)e^{-\alpha L}-2\sqrt{1-\kappa_1}\sqrt{1-\kappa_2}e^{-\frac{\alpha L}{2}}\cos(k_nL)} \quad (5)$$

where E_t and E_d represents the optical fields of the throughput and drop ports respectively. $\beta=kn_{eff}$ is the propagation constant, n_{eff} is the effective refractive index of the waveguide and the circumference of the ring is $L=2\pi R$, here R is the radius of the ring. In the following, new parameters will be used for simplification: $\varphi=\beta L$ is the phase constant. The chaotic noise cancellation can be managed by using the specific parameters of the add/drop device, which the required signals can be retrieved by the specific users. $\kappa_1$and κ_2 are coupling coefficient of add/drop filters, $k_n=2\pi/\lambda$ is the wave propagation number for in a vacuum, and where the waveguide (ring resonator) loss is $\alpha=0.5$ dB mm^{-1}. The fractional coupler intensity loss is $\gamma=0.1$. In the case of add/drop device, the nonlinear refractive index is neglected.

In operation, the large bandwidth signal within the micro ring device can be generated by using a soliton pulse input into the nonlinear micro ring resonator. This means that the broadband light spectra can be generated after the soliton pulse is input into the ring resonator system. The schematic diagram of the proposed system is as shown in Fig. 1. A soliton pulse with 50 ns pulse width, peak power at 2 W is input into the system. The suitable ring parameters are used, for instance, ring radii $R_1=15.0$ μm, $R_2=10.0$ μm, $R_3=R_s=5.0$ μm and $R_5=R_d=20.0$ μm as shown in Fig. 2. In order to make the system associate with the practical device [3], the selected parameters of the system are fixed to $\lambda_0=1.55$ μm, $n_0=3.34$ (**InGaAsP/InP**), $A_{eff}=0.50$, 0.25 and 0.10 μm^2 for a micro and nano ring resonator, respectively, $\alpha=0.5$ dB mm^{-1}, $\gamma=0.1$. The coupling coefficient (kappa, κ) of the micro ring resonator ranged 0.1–0.96. The nonlinear refractive index is $n_2=2.2\times10^{-13}$ m^2/W. In this case, the wave guided loss used is 0.5 dB mm^{-1}. The input soliton pulse is chopped (sliced) into the smaller signals spreading over the spectrum as shown in Figs. 2(b) and 3(b), which is shown that the large bandwidth signal is generated within the first ring device. The biggest output amplification is obtained within the nano-waveguides (rings R_3 and R_4) as shown in Figs. 2(d), (e) and (f), 3(d), (e) and (f), whereas

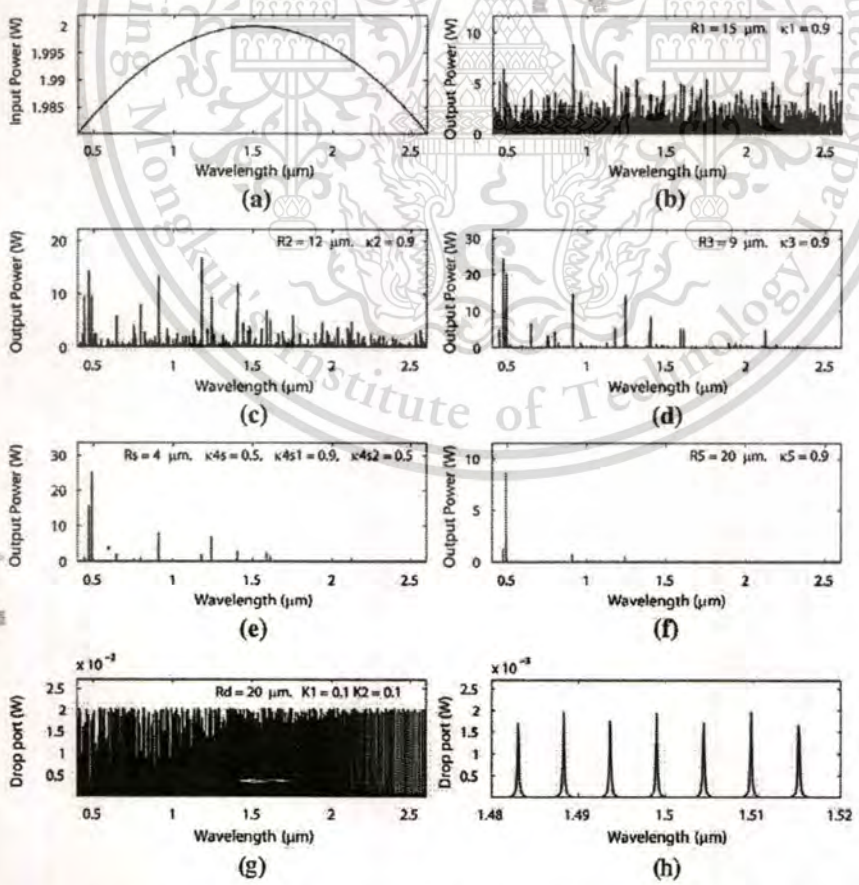

Fig. 3. Results obtained with the storage wavelength at 1.50 μm, where (a) input soliton, (b) ring R_1 and (c) ring R_2, (d) ring R_3, (e) storage ring (R_s), (f) ring R_5, (g) and (h) drop port signals.

Please cite this article as: W. Siririth, et al., Novel storage and tunable light source generated by a soliton pulse in a micro ring resonator system, Opt. Int. J. Light Electron. Opt. (2009), doi:10.1016/j.ijleo.2009.11.005

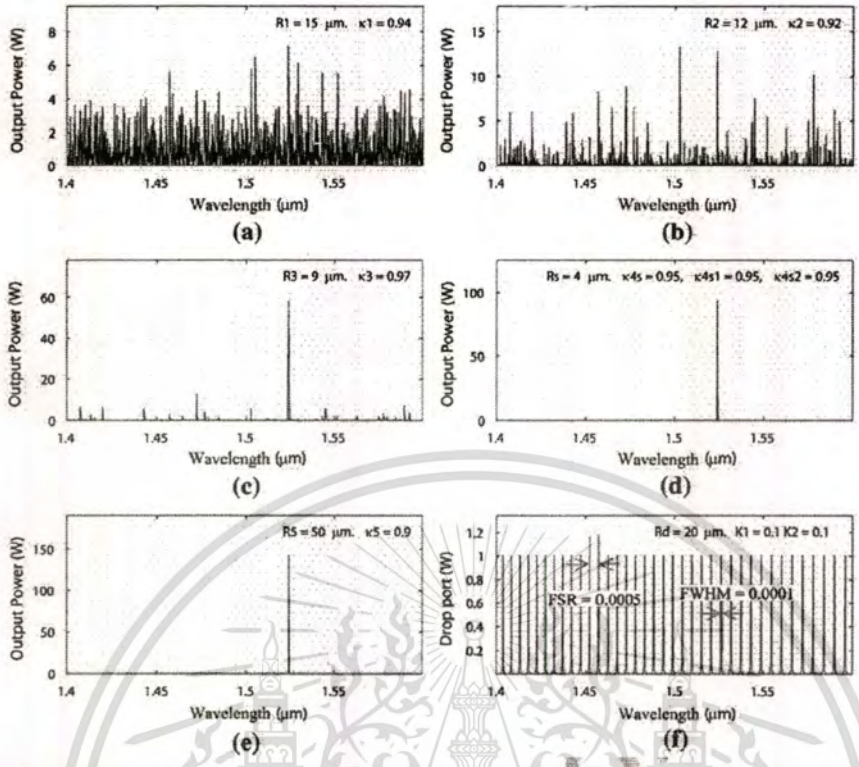

Fig. 4. Results obtained with the storage wavelength at 1.52 μm, where (a) ring R_1 and (b) ring R_2, (c) ring R_3, (d) storage ring R_s, (e) ring R_5 and (f) drop port signals.

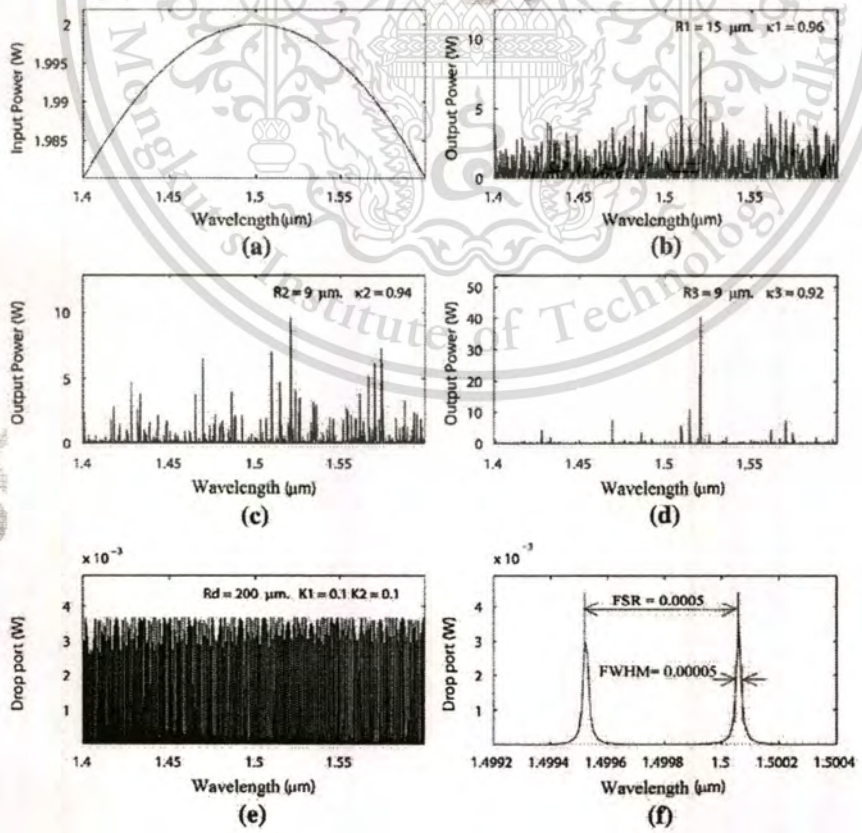

Fig. 5. Results obtained with the storage wavelength at 1.50 μm, where (a) input soliton, (b) ring R_1 and (c) ring R_2, (d) ring R_3 and (f) drop port signals.

Please cite this article as: W. Siririth, et al., Novel storage and tunable light source generated by a soliton pulse in a micro ring resonator system, Opt. Int. J. Light Electron. Opt. (2009), doi:10.1016/j.ijleo.2009.11.005

the maximum power of 10 W is obtained at the center wavelength of 1.50 and 0.50 μm, respectively. The coupling coefficients are given as shown in the figures. The coupling loss is included due to the different core effective areas between micro and nano ring devices, which is given by 0.1 dB.

In conclusion, we have shown that a broadband light source at the specific center wavelength can be generated, stored and regenerated. The storage of broadband light source within a storage ring (R_s or R_4) is achieved, which has also been confirmed by Ref. [4]. The maximum stored power of 100 W is obtained as shown in Fig. 4(d), where the average optical output power of 4.0 W is achieved via an add/drop filter as shown in Fig. 5(f). The spectral width, i.e. full width at half maximum (FWHM) and free spectrum range (FSR) of 50 and 500 pm are obtained as shown in Fig. 5(f), which is allowed the increasing in channel capacity of 10,000 times in a single center wavelength. In application, the problem of the signal interference, i.e. collision, can be managed by using the appropriate free spectrum range design [7].

References

[1] P.P. Yupapin, N. Pornsuwanchroen, S. Chaiyasoonthor, Attosecond pulse generation using nonlinear micro ring resonators, Microwave Opt. Technol. Lett. 50 (12) (2008) 3108–3111.

[2] N. Pornsuwancharoen, P.P. Yupapin, Generalized fast, slow, stop, and store light optically within a nano ring resonator, Microwave Opt. Technol. Lett. 51 (4) (2009) 899–902.

[3] Y. Su, F. Liu, Q. Li, System performance of slow-light buffering and storage in silicon nano-waveguide, Proc. SPIE 6783 (2007) 68732P.

[4] P.P. Yupapin, N. Pornsuwanchroen, Proposed nonlinear micro ring resonator arrangement for stopping and storing light, IEEE Photonics Technol. Lett. 21 (2009) 404–406.

[5] P.P. Yupapin, W. Suwancharoen, Chaotic signal generation and cancellation using a micro ring resonator incorporating an optical add/drop multiplexer, Opt. Commun. 280/2 (2007) 343–350.

[6] N. Pornsuwancharoen, S. Chaiyasoonthorn, P.P. Yupapin, Fast and slow lights generation using chaotic signals in the nonlinear micro ring resonators for communication security, Opt. Eng. 48 (1) (2009)50005-1-5 48 (1) .

[7] P.P. Yupapin, P. Saeung, C. Li, Characteristics of complementary ring-resonator add/drop filters modeling by using graphical approach, Opt. Commun. 272 (2007) 81–86.

Please cite this article as: W. Siririth, et al., Novel storage and tunable light source generated by a soliton pulse in a micro ring resonator system, Opt. Int. J. Light Electron. Opt. (2009), doi:10.1016/j.ijleo.2009.11.005

BIOGRAPHY

Date of Birth: July 13th, 1974

Born: Bangkok Province, Thailand

Current Address: 37/87 Moo 8, Tambol Bangkrasor, Amphur Muang, Nonthaburi, Thailand, 11000.

E-mail: siririth@gmail.com , x_siririth@yahoo.com

Education

- Bachelors of Engineering in Electrical Engineering, Faculty of Engineering, Mahanakorn University of Technology, Bangkok, Thailand, in 1997.
- Master of Engineering in Electrical Engineering, Faculty of Engineering, Mahanakorn University of Technology, Bangkok, Thailand, in 2002.

Experience

- 3 years in Lecturer of Faculty of Engineering, Rajapark College, Bangkok, Thailand.
- 4 years in Lecturer of Department of Electrical Engineering, Faculty of Engineering, Eastern Asia University, Bangkok, Thailand.
- 5 years in Lecturer of Department of Computer Engineering, Faculty of Engineering, Chiang Rai College, Chiang Rai, Thailand.

Skilled Works

- Theory of Computation
- Artificial Intelligence
- Neural Network & Fuzzy Set
- Nonlinear Optical, Optical Device Design & Simulation